Int J Earth Sci (Geol Rundsch)
DOI 10.1007/s00531-010-0585-3

ORIGINAL PAPER

The Early Palaeozoic high-grade metamorphism at the active continental margin of West Gondwana in the Andes (NW Argentina/N Chile)

Friedrich Lucassen · Raúl Becchio · Gerhard Franz

Received: 16 December 2009 / Accepted: 28 July 2010

Abstract The evolution of the Early Palaeozoic orogen of West Gondwana in the Cambrian to Ordovician basement of the Andes between ~18° and 32° S is investigated for pressure and temperature conditions and age of metamorphism. It is characterized by mid-crust temperatures commonly above the wet granite solidus (~650°C). Widespread felsic migmatite and rare granulite formed at pressures of ca 0.5–0.7 GPa, locally 1.0 GPa. These rocks represent the deepest exhumed sections of the Early Palaeozoic crust. High pressure–low temperature rocks are absent. The crystallization ages, compiled from the literature in combination with new data, for near peak metamorphic conditions of these high-grade metamorphic rocks in NW Argentina and N Chile are ~530–500 Ma and ~470–420 Ma. Both age groups are spatially overlapping. Radiogenic isotope signatures (Sr, Nd, Pb) are used to characterize the Early Palaeozoic basement. The Pb and Sr isotope compositions of the Early Palaeozoic basement indicate mixing arrays between pre-Palaeozoic unradiogenic and radiogenic crust. Crustal residence ages (Sm–Nd T_{DM}) indicate a prominent event of crust formation around ~2 Ga, which is known continent-wide. This material was recycled during Midproterozoic and Early Palaeozoic orogenies without prominent additions of new crust present in the isotope record, i.e. accretion of compositional exotic material is absent.

Keywords Active continental margin · Orogeny · *P–T–t* · Crustal composition · Central Andes · Early Palaeozoic

Introduction

The Pacific margin of the Central Andes was active over long periods in the Early and Late Palaeozoic and from the Mesozoic onwards (e.g. Coira et al. 1982; Ramos 2000). At the latitude of the Puna (22–26°S), the continental margin throughout the Neoproterozoic and Phanerozoic formed either during prolonged phases of subduction without collision of continental fragments (e.g. Damm et al. 1990, 1994; Franz et al. 2006) or by cycles of extension, basin formation, rifting and drifting of continental fragments (terranes) and re-accretion of the terranes during subduction (for a summary see Ramos 2008). The accretion of terranes exotic to this margin (the Argentine Precordillera, Chilenia, and Mejillonia terranes) is debated for the area west of the Neoproterozoic to Early Palaeozoic orogens (e.g. Ramos et al. 1986; Rapela et al. 1998; Aceñolaza et al. 2002; Astini and Dávila 2004; Finney et al. 2005; Ramos 2008; Willner et al. 2008). The Neoproterozoic to Ordovician orogens (Fig. 1) formed part of the worldwide Brasiliano-Panafrican orogenic belts, which evolved during Neoproterozoic and Early Palaeozoic time (e.g. Cawood and Buchan 2007). Early Palaeozoic metamorphism and magmatism (~570–420 Ma) were traced by radiogenic isotope

Electronic supplementary material The online version of this article (doi:10.1007/s00531-010-0585-3) contains supplementary material, which is available to authorized users.

F. Lucassen (✉)
Deutsches GeoForschungsZentrum,
Telegrafenberg, 14473 Potsdam, Germany
e-mail: lucassen@gfz-potsdam.de

F. Lucassen · G. Franz
Technische Universität Berlin, Fachgebiet Petrologie,
Ackerstr. 71–76, 13355 Berlin, Germany

R. Becchio
Universidad Nacional de Salta-Instituto GEONORTE
and CONICET-INENCO, Av. Bolivia 5150,
Salta 4400, Argentina

Published online: 18 August 2010

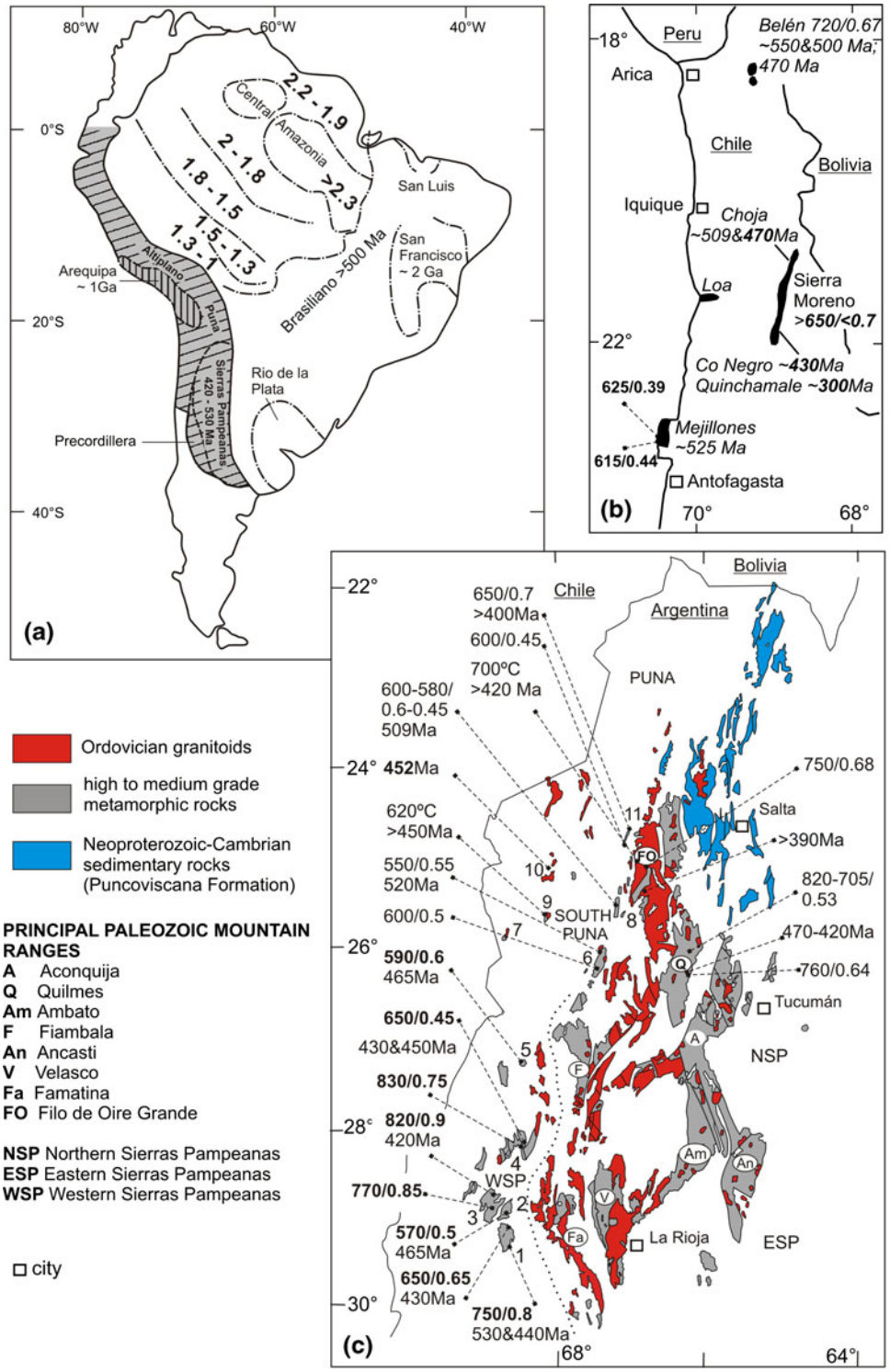

geochronology from ~4°S–42°S along the western margin and inland of the South American continent (Fig. 1a; e.g. Damm et al. 1990, 1994; Pankhurst et al. 1998, 2000 and 2006; Sims et al. 1998; Lucassen et al. 2000; Wörner et al. 2000; Lucassen and Becchio 2003; Büttner et al. 2005; Steenken et al. 2006, 2008; Chew et al. 2007; Viramonte et al. 2007; Schwartz et al. 2008; Siegesmund et al. 2010; Casquet et al. 2010). Fossil thermal regimes of exhumed orogens are revealed by quantitative studies of metamorphic and magmatic rocks including pressure–temperature conditions, crystallization ages and chemical and isotopic compositions in the regional geological context.

◀ **Fig. 1** **a** Growth pattern of South America showing the core regions of the craton and younger tectono-magmatic–metamorphic provinces (after Cordani et al. 2003, 2009). The western Pacific margin is dominated by variable reworking of older material during the Phanerozoic and in the Early Palaeozoic and ongoing Cenozoic subduction related orogens, respectively. Such old material is represented e.g. by the Arequipa domain with Sunsas (Grenville) crystallization age (e.g. Wasteneys et al. 1995; Wörner et al. 2000; Casquet et al. 2010). The most prominent exposures of the Early Palaeozoic orogen are in the Sierras de Pampeanas (e.g. in: Pankhurst and Rapela 1998) and the southern Puna Plateau (e.g. Damm et al. 1994; Becchio et al. 1999; Lucassen et al. 2000). Occurrences of Early Palaeozoic magmatic and metamorphic rocks extend into Chile, Peru and southern Ecuador (*diagonal ruling*; e.g. Damm et al. 1994; Lucassen et al. 2000; Chew et al. 2007, 2008). **b** Early Palaeozoic metamorphic rocks in N Chile occur in Belén (Wörner et al. 2000), Rio Loa cañón, Mejillones Peninsula and Sierra de Moreno (Lucassen et al. 2000). New age data presented in this study are from Quebrada Choja, Cerro Negro and Quebrada Quinchamale of the Sierra de Moreno. *P–T* estimates (in °C/GPa) from Mejillones are from this study, others from the literature. **c** *P–T* estimates (in °C/GPa) of peak metamorphic conditions in the high-grade basement of NW Argentina (this study *in bold letters*; other data from Becchio 2000); age data are U–Pb ages on titanite (Lucassen and Becchio 2003; Büttner et al. 2005; this study) and minimum ages of metamorphism from K–Ar dating on minerals marked by '>'xxx Ma (Lucassen et al. 2000). The geological map (after SEGEMAR 1997) shows the distribution of Palaeozoic magmatic–metamorphic rocks and Neoproterozoic–Cambrian sedimentary rocks (Puncoviscana Formation) in the principal Palaeozoic Mountain Ranges between ~22°S and 30°S. Locations with new *P–T* data, geochemistry or age determinations are presented in detail in the text. The key to the locations from south to north is: (*1*) Maz, (*2*) Espinal, (*3*) Umango, (*4*) Toro Negro, (*5*) Cazadero Grande, (*6*) El Peñón/El Jote, (*7*) Cerro Plegado, (*8*) Hombre Muerto, (*9*) Antofalla, (*10*) Archibarca, (*11*) Centenario

We present new quantitative pressure–temperature estimates of the peak-metamorphic mineral paragenesis between ~29°S and 23°S, element geochemical and Nd, Pb, and Sr isotope data of 34 Cambrian to Ordovician high-grade metamorphic rocks between ~29°S and 27°S. Five new U–Pb ages on titanite in high-grade metamorphic rocks (Sierra de Moreno/North Chilean Precordillera; Fig. 1b) and from the Archibarca granite (Salar de Antofalla; NW Argentina; Fig. 1c) supplement existing age data (Lucassen and Becchio 2003 and references therein). The new data provide insights into the thermal, time and compositional structure of the Palaeozoic orogen from the Pacific coast to the eastern slope of the present Andes together with the existing data base.

Early Palaeozoic high-grade metamorphic rocks between 18 and 32°S

In the study area, the Neoproterozoic to Cambrian Pampean and Ordovician to Silurian (in parts transitional to Devonian) Famatinian orogenies (or cycles) were distinguished in the Palaeozoic orogen mainly on the base of ages of sedimentation and magmatism (defined by Aceñolaza and Toselli 1976; see also Miller et al. 1994; Rapela et al. 1998; Pankhurst et al. 1998, 2000). Pampean and Famatinian metamorphic crystallization ages of high-grade metamorphic and crust-dominated magmatic rocks overlap regionally and occur in the same areas especially in the western sections of the orogen (for recent reviews see Lucassen et al. 2000; Pankhurst et al. 2000; Lucassen and Becchio 2003). The Palaeozoic orogen is well exposed in northwest and central Argentina in what is now the southern high plateau or the Andean back arc and stretches in scattered outcrops as far west as the north Chilean coast (Fig. 1).

High-grade metamorphism of the high-temperature–low to medium-pressure type (~600–750°C, 0.4 to 0.8 GPa) is common and independent of the variable crystallization ages (~530–500 Ma and ~470–450 Ma; e.g. Grissom et al. 1991, 1998; Rapela et al. 1998; Becchio et al. 1999; Lucassen et al. 2000; Wörner et al. 2000; Porcher et al. 2004; Büttner et al. 2005; Casquet et al. 2006; Viramonte et al. 2007; Otamendi et al. 2008). Abundant felsic migmatites indicate similar conditions, i.e. temperatures above the wet granite solidus (Johannes and Holtz 1996), in areas where quantitative thermo-barometry is not available. The common metamorphic basement of NW Argentina (Fig. 1) comprises rocks of felsic composition with little variation in their lithologies. Most rocks have siliciclastic sedimentary protoliths with compositions between quartz-feldspar-rich greywackes and shales as endmember. Transitions from low grade, likely Neoproterozoic to Cambrian sedimentary rocks to migmatites and rare granulite, are observed in the Puncoviscana Formation (e.g. Büttner et al. 2005). Less common orthogneisses formed from granodiorite–granite intrusions. Marbles, calcsilicate rocks, and amphibolites (meta-dikes/lavas and meta-gabbros) are of minor volume in general but can be locally dominant. Their thickness varies between decimetres and tens to hundred of metres within the dominant gneiss-migmatite unit, and all rocks indicate a similar metamorphic grade at the outcrop scale (detailed descriptions in Viramonte et al. 2007 and references therein).

The occurrence of high-grade Early Palaeozoic metamorphic basement in Northern Chile is restricted to a few outcrops in the coastal area, the Chilean Precordillera, and the western slope of the Altiplano (Península Mejillones, cañón del Río Loa, Sierra de Moreno, Belén; Fig. 1b). In comparison with NW Argentina, the appearance and element and isotope compositions of the metamorphic rocks are similar, but pelite and carbonate protoliths are rare, however, (Lucassen et al. 1999a, 2001). Detailed descriptions of the Chilean outcrops have been given previously (Lucassen et al. 2000; Wörner et al. 2000 and references therein).

Geo-thermo-barometry and age determinations

Titanite, a common accessory mineral in metamorphic rocks at moderate pressures and especially in calcsilicate rocks, is here used for U–Pb dating and yields crystallization ages (e.g. Romer and Rötzler 2001). Sample preparation, chemistry and mass spectrometric procedures are in the eAppendix. The new data include four metamorphic rocks from N Chile.

Table 1 gives an overview of *P–T* conditions in NW Argentina and N Chile, on the basis of geo-thermobarometers mostly including garnet (mineral data are in eTable 1). For analytical methods of microprobe analyses, major and trace element determinations and Sr, Nd, Pb isotope ratios on whole rocks see the eAppendix. We focus on the peak metamorphic conditions and will show that these are rather similar over the extended area of several hundred km (Fig. 1b, c). Information about the prograde evolution is not preserved in the high *T* samples. Core-rim relations in garnet always indicate a clockwise *P–T* path and no indications for anti-clockwise development were found. Details about prograde or retrograde development require the investigation of preferably complete sections including the lower-grade metamorphic rocks (e.g. in Sierra de Quilmes; Büttner et al. 2005; Büttner 2009; Fig. 1c) and will probably differ from one locality to the other due to different tectonic development.

Figure 1c shows the distribution of *P–T–t* in the study area in NW Argentina. From the southern Puna Plateau to the Sierras Pampeanas, the estimated peak metamorphic conditions are ca 600–870°C and ca 0.4–1.0 GPa with a mean value of 0.65 GPa. Ages of metamorphic crystallization are 530–420 Ma without a well constraint regional distribution pattern (Lucassen and Becchio 2003). Similar rock types, metamorphic conditions and crystallization ages are described from the scattered and scarce Chilean outcrops (e.g. Damm et al. 1990, 1994; Lucassen et al. 2000; Wörner et al. 2000). In the following, we give a

Table 1 Pressure temperature estimates from mineral chemistry

Sample	Area	Lithology	Mineral paragenesis	Results *T* (°C) *P* (GPa)		Methods
				Core	Rim	
NW Argentina						
01/124	Maz	Orthogneiss	Grt-Pl-Amp	750–800/0.8-0.9	640–730/0.7	2, 3, 5
01/101	Maz	Micaschist	Grt-Pl-Bt-Ms-Sil-St	650–700/0.65	560–620/0.5–0.6	4, 9,11
01/94	Umango	Amphibolite	Grt-Pl-Amp	800/0.95	770/0.8	3, 5
01/83b	Umango	Amphibolite	Grt-Pl-Cpx-Kfs	908/1.0	750–820/0.9	2, 3, 5,10
01/66	Espinal	Migmatite	Grt-Pl-Bt-Ms-Sil	570/0.5		9, 10
01/57	Toro Negro	Amphibolite	Grt-Pl-Amp	650/0.45	615/0.4	3, 5
01/56	Toro Negro	Migmatic gneiss	Pl-Grt-Sil-Bt-Ms	830/0.75	650/0.5	9, 11
01/45	Cazadero Grande	Amphibolite	Grt-Pl-Amp	590/0.6		3, 5
6/131*	El Peñón	Gneiss	Pl-Ms-Kfs-Qtz	550/0.45–0.55		7
6/129*	El Peñón	Mica schist	Grt-Bt-Pl-Kfs-Qtz	550–600/0.50		1, 4
150IIc*	Quilmes	Migmatite	Grt-Bt-Pl-Ms-Kfs-Qtz	590–705/0.53	470–520/0.33	1, 4
150IIIc*	Quilmes	Migmatite	Grt-Bt-Pl-Ms-Kfs-Qtz	640–820/0.53	450–520/0.32	1, 4
6/111*	Quilmes	Migmatite	Cpx-Opx	700		8
6/110*	Quilmes	Migmatite	Grt-Bt-Pl-Cd-Sil-Qtz	630–760/0.64	590–720/0.52	1, 4
6/139*	El Jote	Amphibolite	Grt-Amp-Pl-Qtz	550–565/0.39		2, 4, 5
4/7*	Hombre Muerto	Migmatite	Grt-Bt-Pl-Ms-Kfs-Qtz	520–580/0.45	550/0.5	1, 4, 7
6/76*	Hombre Muerto	Gneiss	Grt-Bt-Pl-Ms-Kfs-Qtz	570–600/0.45–0.6		1, 4, 7
4/32*	Filo Oire Grande	Migmatite	Grt-Bt-Pl-Sil-Qtz	620–750/0.68	590–660/0.5	1, 4
4/30*	Filo Oire Grande	Amphibolite	Amp-Pl	680–700		3
5/09*	Centenario	Schist	Grt-St-Bt-Sil-Pl-Qtz	590–650/0.7	550/0.5	1, 4
5/19*	Centenario	Gneiss	Grt-Bt-Ms-Pl-And-Qtz	580–600/0.45	550/0.35	1, 4, 6
Northern Chile						
3/373	Mejillones	Amphibolite	Amph-Pl-Grt-Qtz	625/0.39		2, 5
3/385	Mejillones	Gneiss	Amph-Pl-Grt-Qtz	615/0.44	510/0.29	2, 5

* Data from Becchio (2000); key to methods: 1. Kleemann and Reinhardt (1994); 2. Graham and Powell (1984); 3. Holland and Blundy (1994); 4. Berman (1988, 1991); 5. Kohn and Spear (1990); 6. Ghent and Stout (1981); 7. Massonne and Schreyer (1987); 8. Lindsley (1983); 9. Holdaway et al. (1997); 10. Sengupta (1989); 11. Bhattacharya et al. (1989)

summary of the field relations and petrography of the studied basement areas, in combination with the *P–T-t* data.

N Chile

Mejillones peninsula

The occurrence of high-grade metamorphic rocks is restricted to the central part of the peninsula (~23°13′–23°22′S; ~70°33′W; map in: Baeza 1984). The suite is dominated by medium- to coarse-grained (0.5–1 mm) biotite gneiss with minor intercalated amphibolite (few m to 10 m scale). Migmatization is absent (Baeza 1984). Penetrative foliation in a garnet amphibolite and in an amphibole–biotite gneiss formed during peak metamorphism. The mineral assemblage of the amphibolite (sample 3/373) comprises >20 vol% hornblende and garnet, <20 vol% plagioclase and cummingtonite, <10 vol% quartz and biotite as well as accessory (<5 vol%) ilmenite and magnetite. The gneiss (3/385) contains <40% plagioclase, <20 vol% hornblende, garnet and biotite and <5 vol% cummingtonite, muscovite, ilmenite and magnetite. The composition of the silicate minerals is uniform and compositional zoning is absent or restricted to small outer rims (3/385). The application of geo-thermo-barometry to the paragenesis hornblende-garnet-plagioclase-quartz yielded ~0.35 GPa and 625°C in the amphibolite and ~0.44 GPa and 615°C (core) and 0.29 GPa and 510°C (rim) in the gneiss (Table 1; eTable 1 for the microprobe analyses).

The age of the high-grade metamorphism from an internal mineral isochron on a garnet amphibolite (Sm–Nd) is 525 ± 10 Ma (Lucassen et al. 2000). The K–Ar isotope system in hornblende and biotite is influenced by thermal field of the extended Jurassic intrusions and reset to ~150 Ma (Lucassen et al. 2000). The T_{DM} of amphibolite and gneiss is ~1.5 Ga and indicates a Proterozoic age of the magmatic and metasedimentary protoliths (Lucassen et al. 2000).

Sierra de Moreno

The most common rock type is gneiss with varying proportions of feldspar, quartz, biotite and rare garnet and muscovite. The protoliths were greywacke-type sediments as inferred from bulk element chemical composition and compositional layering (Lucassen et al. 1999a, 2000). Calcsilicate rocks, dioritic orthogneiss and amphibolite are scarce and of minor volume. Migmatization has occurred in the metasedimentary rocks and indicates upper amphibolite facies temperatures of >650°. Garnet is rare or absent in mafic amphibolites. It indicates moderate pressure below ~0.5–0.7 GPa. Quantitative geo-thermo-barometry in these rocks is hampered by the lack of suitable mineral paragenesis.

The age of peak metamorphism is not well constraint. Metamorphic rocks from Quebrada Choja in the northern Sierra de Moreno have yielded a variety of ages in the U–Pb system (U–Pb intercept ages: migmatite: ~ 466 Ma, Damm et al. 1990; ~ 470 Ma, Loewy et al. 2004; orthogneiss ~ 415 Ma, Damm et al. 1990; ~ 497 Ma, Loewy et al. 2004). An internal Sm–Nd mineral isochron from a calcsilicate rock from the same location at Quebrada Choja yielded 505 ± 6 Ma and a K–Ar age on hornblende 478 ± 15 Ma (Lucassen et al. 2000). K–Ar ages on amphibole and biotite from high-grade metamorphic rocks vary between ~ 470 Ma in the northern part and ~ 300 Ma in the southern part of Sierra de Moreno. The K–Ar ages were interpreted as cooling ages from peak metamorphism and variably influenced by the thermal field of Late Palaeozoic intrusions in the area (age of the intrusions ~ 300 Ma; Lucassen et al. 1999a, 2000). T_{DM} ages of the metamorphic rocks in Sierra de Moreno are between ~1.6 and 1.9 Ga (Lucassen et al. 2000, 2001).

In order to obtain a more precise age of metamorphism, titanite separates from three calcsilicate and one migmatite sample from Sierra de Moreno have been dated by the U–Pb method (Fig. 2a–d; Table 2). Sample 4/326 is from Quebrada Choja (Fig. 1b; 21°04′32″S; 68°32°44″W) from a lens of coarse-grained calcsilicate rock in migmatite. Samples 3/63 and 3/74 are from dm-thick layers of calcsilicate rock in migmatite from the Cerro Negro area (Fig. 1b; 21°51′43″S; 69°06′55″W). The migmatite 4/76 is from Quebrada Quinchamale (Fig. 1b; 21°52′54″S69°05′52″W) close to the border with a Late Palaeozoic intrusion. Different types of titanite could neither be distinguished in thin section nor be distinguished in the mineral separates under the binocular microscope. Six titanite fractions from calcsilicate sample 4/326 are concordant or near concordant (Fig. 2a) with mean ages of 470.4 ± 7.7 Ma ($^{206}Pb/^{238}U$) and 469.6 ± 5.1 ($^{207}Pb/^{235}U$). This ~470 Ma age is similar to U–Pb intercept ages from zircons in granitoid rocks and migmatite from the same area (Damm et al. 1990; Loewy et al. 2004) but it is distinctly younger than the Sm–Nd mineral isochron of ~505 Ma (Lucassen et al. 2000). Concordant or near concordant titanite fractions of calcsilicate 3/63 (Fig. 2b; Table 2) yielded average ages of 432.1 ± 3.7 Ma ($^{206}Pb/^{238}U$) and 433.4 ± 2.8 Ma ($^{207}Pb/^{235}U$). Titanite separates from calcsilicate 3/74 show a range of concordant ages between ~440 and ~410 Ma (Fig. 2c; Table 2). Spread of ages along the concordia is commonly attributed to small Pb loss or inheritance of radiogenic Pb from precursor minerals, which especially

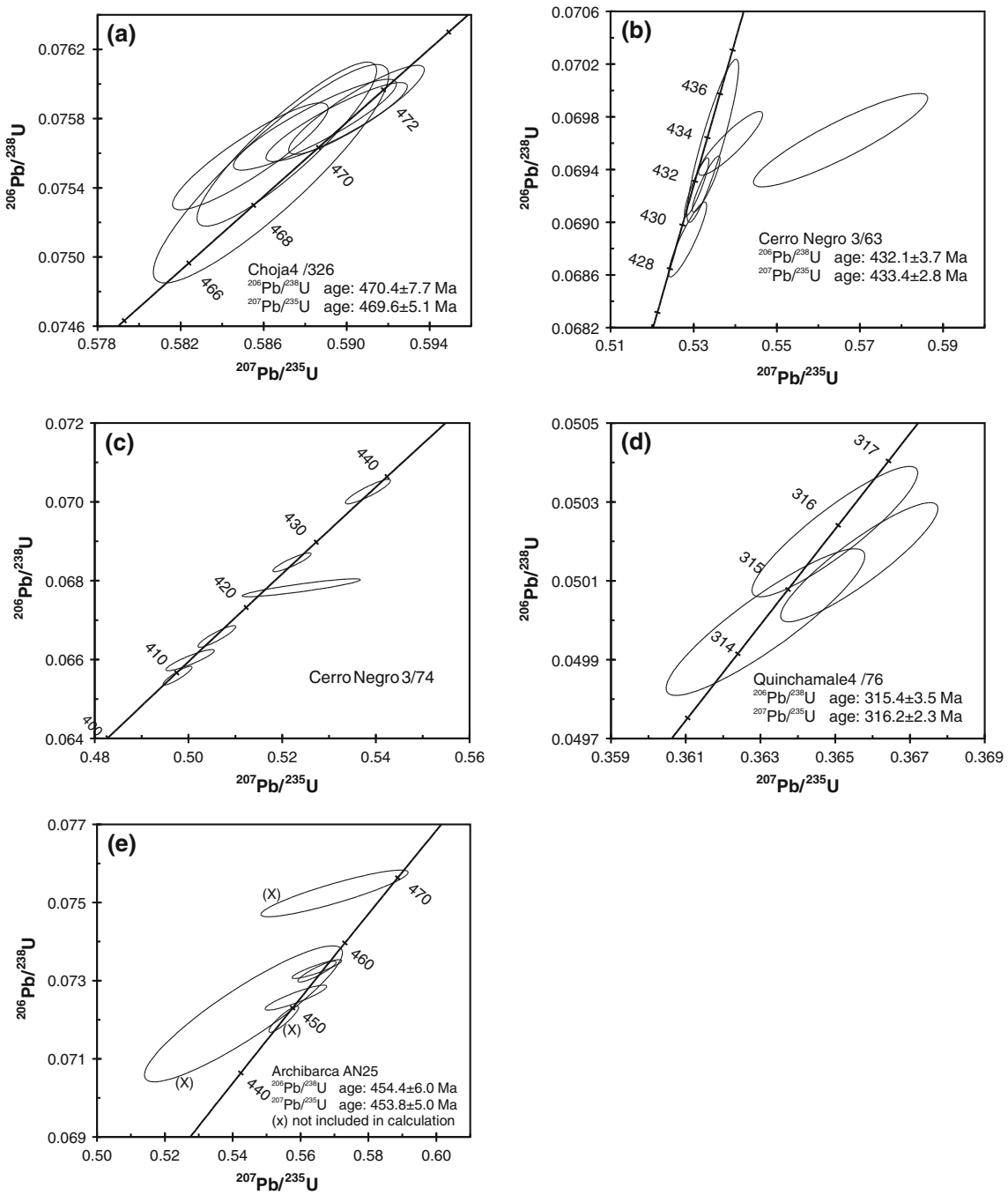

Fig. 2 Concordia diagrams for titanite from the different samples (**a**–**d**) from Sierra de Moreno/N Chile and (**e**) Archibarca/NW Argentina. Sample locations are indicated in Fig. 1. Data-point error ellipses are 2σ. The figure was plotted using ISOPLOT (vers. 2.49; Ludwig 2001)

affects low μ ($\mu < 2{,}000$; $\mu = {}^{238}U/{}^{204}Pb$) minerals (e.g. Romer 2001; Romer and Rötzler 2005). Considering the old concordant ~470 Ma age from Quebrada Choja and the young ~430 Ma age from Cerro Negro, the range of ages from 3/74 could be caused by inheritance of radiogenic Pb (the apparent older ages in Fig. 2c) from precursor titanite during younger titanite growth.

The migmatite (4/76; Table 2) with average ages of 315.4 ± 3.5 Ma ($^{206}Pb/^{238}U$) and 316.2 ± 2.3 Ma ($^{207}Pb/^{235}U$) is distinctly younger than titanite from the other samples and belongs to the thermal event in the crust that is documented by the abundant Late Palaeozoic magmatism in the Coastal and Precordillera of northern Chile (e.g. Maksaev 1990; Lucassen et al. 1999a). The same migmatite sample

Table 2 Results of U–Pb dating on titanite

Sample	Location rock type	Wt (m)	Pb (ppm)	U (ppm)	Isotopic ratios				Ages (in Ma)		
					$^{206}Pb/^{204}Pb^{(a)}$	$^{207}Pb/^{206}Pb$	$^{206}Pb/^{238}U$	$^{207}Pb/^{235}U$	$^{206}Pb/^{238}U$	$^{207}Pb/^{235}U$	$^{207}Pb/^{206}Pb$
	Chile										
4-326(1)	Qda. Choja	0.413	11.1	105	320	0.05643	0.0755	0.5874	469.7 ± 5.2	467.9 ± 3.3	459.1 ± 4.1
4-326(2)		0.594	10.8	96.4	281	0.05663	0.0757	0.5908	470.8 ± 3.7	469.9 ± 2.6	465.5 ± 3.2
4-326(3)		0.608	11.0	109	344	0.05652	0.0756	0.5890	470.1 ± 3.7	469.0 ± 2.5	463.7 ± 3.0
4-326(4)	Calcsilicate	0.579	10.2	97.8	347	0.05666	0.0757	0.5914	470.9 ± 4.6	470.6 ± 3.2	469.0 ± 3.8
4-326(5)		0.522	10.0	92.7	275	0.05676	0.0758	0.5929	471.3 ± 3.9	471.2 ± 2.4	470.5 ± 3.1
4-326(6)		0.526	10.1	96.7	303	0.05661	0.0754	0.5885	469.1 ± 4.2	468.5 ± 2.7	465.8 ± 3.3
Mean age									470.4 ± 7.7	469.6 ± 5.1	
3-63(1)	Co Negro	0.365	17.9	140	150	0.05566	0.0689	0.5285	429.3 ± 2.0	430.8 ± 1.3	438.9 ± 1.8
3-63(2)		0.388	17.5	144	234	0.05889	0.0696	0.5654	433. ± 6.3	455.0 ± 8.1*	563.1 ± 8.2
3-63(3)		0.458	17.7	142	202	0.05569	0.0696	0.5346	433.9 ± 2.5	434.9 ± 1.9	440.1 ± 2.4
3-63(4)	Calcsilicate	0.549	18.5	157	220	0.05557	0.0693	0.5307	431.7 ± 1.8	432.3 ± 1.3	435.2 ± 1.7
3-63(5)		0.456	21.6	150	111	0.05615	0.0696	0.5389	433.7 ± 1.7	437.7 ± 1.6	458.5 ± 1.9
3-63(6)		0.527	18.4	153	221	0.05579	0.0693	0.5330	431.9 ± 2.1	433.8 ± 1.5	444.1 ± 2.1
Mean age									432.1 ± 3.7	433.4 ± 2.8	
3-74(1)	Calcsilicate	0.614	5.17	54.4	216	0.05499	0.0660	0.5004	411.9 ± 4.4	411.9 ± 2.7	412.0 ± 3.1
3-74(2)		0.656	5.16	54.1	233	0.05512	0.0666	0.5060	415.6 ± 4.4	415.8 ± 2.6	417.0 ± 3.2
3-74(3)		0.443	6.24	64.8	279	0.05557	0.0703	0.5383	437.7 ± 6.8	437.3 ± 4.1	435.2 ± 5.0
3-74(4)		0.308	4.89	54.3	291	0.05530	0.0685	0.5221	426.9 ± 12	426.5 ± 6.7	424.6 ± 8.1
3-74(5)		0.550	9.16	59.4	76	0.05604	0.0678	0.5241	423.0 ± 1.9	427.9 ± 1.7	454.1 ± 1.9
3-74(6)		0.431	5.39	60.7	267	0.05503	0.0656	0.4977	409.6 ± 6.8	410.1 ± 3.7	413.3 ± 4.6
Mean age											
4-76(1)	Quinchamale	0.122	8.92	94.6	206	0.05288	0.0501	0.3656	315.4 ± 1.2	316.4 ± 0.9	323.8 ± 1.3
4-76(2)		0.405	8.37	90.1	245	0.05268	0.0500	0.3631	314.5 ± 4.5	314.6 ± 2.4	315.0 ± 4.1
4-76(3)	Migmatite	0.492	8.72	94.4	246	0.05271	0.0502	0.3650	315.9 ± 3.5	315.9 ± 1.9	316.2 ± 3.2
Mean age									315.4 ± 3.5	316.2 ± 2.3	
	Argentina										
AN25(1)	Archibarca	0.475	16.7	106	205	0.05583	0.0726	0.5586	451.6 ± 3.8	450.6 ± 3.5	445.8 ± 3.8
AN25(2)		0.249	20.8	129	166	0.05589	0.0733	0.5648	456.0 ± 3.7	454.7 ± 2.6	448.0 ± 3.5
AN25(3)		0.396	16.3	111	256	0.05460	0.0722	0.5432	449.1 ± 9.5*	440.5 ± 10.9*	395.6 ± 8.4
AN25(4)	Granodiorite	0.456	14.2	91.7	185	0.05590	0.0720	0.5550	448.3 ± 2.8*	448.3 ± 1.7*	448.4 ± 2.7
AN25(5)		0.312	20.9	109	96	0.05495	0.0752	0.5700	467.6 ± 3.2*	458.0 ± 3.5*	410.2 ± 2.9
AN25(6)		0.278	20.6	128	201	0.05594	0.0732	0.5648	455.6 ± 3.8	454.7 ± 2.5	450.0 ± 3.6
Mean age									454.4 ± 6.0	453.8 ± 5.0	

(a) measured ratio corrected for mass fractionation of (0.1 ± 0.05)% per a.m.u.; all other isotope ratios are also corrected for spike composition, blank (Pb: 15 pg ± 7.5; U: 1 pg ± 0.5), and common lead composition using Pb isotope composition of feldspar from Early Palaeozoic metamorphic rocks (average of 7 samples: $^{206}Pb/^{204}Pb$ 18.59, $^{207}Pb/^{206}Pb$ 15.85; Lucassen et al. 2002). Errors of the weighted mean ages of samples 4/326, 3/63, 4/76, and AN25 are at the 95% confidence level. * Not included in the average

was previously dated at 311 ± 7 Ma by K–Ar on hornblende (Lucassen et al. 2000, 2001) and the combination of titanite and hornblende ages points to rapid cooling. This migmatite likely was related to contact metamorphism in the vicinity of the Late Palaeozoic intrusions.

NW Argentina: southern Puna

Metamorphic *P–T* conditions are summarized in Table 1 and Fig. 1c and crustal residence ages T_{DM} of the protoliths from this work are listed in eTable 2. Age data from the sample localities are previously published U–Pb ages on titanite (Lucassen and Becchio 2003) except for one new U–Pb age determination on titanite from the Archibarca granitoid (Table 2). It is included here, because it contributes to the knowledge of the poorly known basement in one of the name-giving areas of the Arequipa-Antofalla terrane (e.g. Loewy et al. 2004).

Archibarca

The Archibarca granitoid is located at the NW border of Salar de Antofalla (25°18′S; 67°47′W). It comprises mainly granite with smaller associated bodies of tonalite to granodiorite. The host rocks are gneisses and minor amphibolite, which previously have been dated by K–Ar mineral ages to ~450–430 Ma ca 30 km south of the intrusion (Kraemer et al. 1999; Lucassen et al. 2000). The granitoids have been dated by K–Ar on minerals to 485 ± 15 Ma (Palma et al. 1986). Sample AN 25 is a fine-grained granodiorite from one of the smaller satellite intrusions of the Archibarca granitoid. Rare phenocrysts are plagioclase, quartz and fine-grained titanite. A scatter of concordant or near concordant U–Pb ages along the concordia between ~470 and ~450 Ma (Fig. 2e; Table 2) could indicate inheritance of older radiogenic Pb or slight Pb loss. Most ages are between 450 and 460 Ma. The average of three of six titanite fractions yielded 454.4 ± 6.0 Ma ($^{206}Pb/^{238}U$) and 453.8 ± 5.0 Ma ($^{207}Pb/^{235}U$). This apparent age is slightly younger than that of nearby Ordovician intrusions of similar composition (Complejo Igneo Pocitos ~470 Ma; Kleine et al. 2004) but within the range of activity of the Famatinian magmatic arc (e.g. in Pankhurst and Rapela 1998). T_{DM} of the Archibarca granitoid is ~1.1 Ga and similar to the nearby Ordovician intrusions (Kleine et al. 2004), whereas the metamorphic rocks from the Antofalla area yielded ~1.9 Ga (Lucassen et al. 2001).

El Peñon

Samples were taken at 26°27′S; 67°14′W. The unit is deformed in prominent shear zones of 1–10 m (in extreme cases 100 m) width with large boudin-like bodies of marble and orthogneiss. Compositional layering (mm-cm scale) of polygonal quartz–feldspar and clinopyroxene–hornblende–epidote–titanite-rich layers marks the foliation plane in the shear zones. In calcsilicate (01/22 with >30% plagioclase and <30% quartz; <10% clinopyroxene, epidote, hornblende, calcite; <3% garnet, titanite), shear bands (mm-scale) mark the foliation by grain size reduction. The shear bands have the same mineral assemblage as the low-strain areas. *P–T* in gneiss and micaschist reached ~550–600°C and 0.5 GPa (Becchio et al. 1999; Becchio 2000). The average age of the metamorphism from three samples is ~520 Ma. The T_{DM} of the calcsilicate (01/22) is 2.0 Ga (eTable 2).

Cerro Plegado

The area is dominated by a series of granitic–dioritic orthogneisses and amphibolite, intruded by a small monzogranite. Contacts between intrusion and metamorphic rocks show ductile deformation. An orthogneiss (AN3-39, from 25°59′S; 68°19′W) composed of plagioclase, potassic feldspar, quartz, biotite and hornblende, with peak-metamorphic epidote and titanite, yielded an age of metamorphism of ~465 Ma; the T_{DM} is 1.3 Ga (eTable 2). *P–T* determinations could not be carried out because suitable mineral assemblages are lacking.

Cazadero Grande

Impure marble and calcsilicate rocks occur together with minor amphibolite in boudins (m to 10 s of m-scale) within migmatite (samples taken at 27°19′S; 68°10′W). Decimetre-scale intercalations of marble, amphibolite, schist and quartzite are locally preserved in the migmatic gneiss and indicate a sedimentary protolith. Garnet-bearing biotite schist has <10% plagioclase, 40–50% quartz, <30% biotite, <10% muscovite and <5% garnet. Metamorphic conditions were 590°C and 0.6 GPa (Table 1) in thin bands (5–10 cm) of amphibolite (01/45) composed of plagioclase, amphibole and garnet. The age of metamorphism is ~450 Ma (two calcsilicate rocks). The T_{DM} ages (eTable 2) are 1.7 Ga (impure marble; sample 01/35) and 1.8 Ga (gneiss; sample 01/36).

NW Argentina: western Sierras Pampeanas

Sierra Toro Negro

The unit of migmatite and minor marble, calcsilicate and amphibolite is very similar to the rocks at Cazadero Grande. Samples were taken at 28°18′S; 68°13′W. The

calcsilicate rock is a layered (mm to cm-scale, 01/54) m-sized boudin. The bright layers (potassic feldspar, plagioclase, clinopyroxene, and minor quartz in variable modes) have a well-annealed polygonal equigranular fabric similar to the dark layers (epidote, clinopyroxene, plagioclase, amphibole, and quartz in variable modes). Both layers contain small amounts of calcite and titanite. The surrounding migmatite (01/55, 01/56, 01/62) has a well-developed foliation marked by the preferred orientation of biotite and variable modes of biotite, quartz and feldspar. Feldspar and quartz form polygonal fabrics. Minor garnet occurs in most samples, sillimanite and/or potassic feldspar, plagioclase and cordierite is present in some samples. Peak metamorphic conditions were 830°C and 0.75 GPa. The retrograde rim compositions yielded 650°C and 0.5 GPa (determined on migmatite 01/56, and on amphibolite 01/57; Table 1). The ages of metamorphism are ~450 and ~430 Ma. The T_{DM} ages (eTable 2) are 1.9 Ga (calcsilicate rock 01–54) and 1.7 and 2.1 Ga (migmatites 01/55, 01/62).

Sierra Espinal

Samples were taken at 28°56′S; 68°17′W. Migmatite with calcsilicate boudins of ~10 m size and some amphibolites (not associated with the calcsilicate rocks) is the dominant lithology. The calcsilicate rocks consist mostly of epidote with minor amounts of clinopyroxene, calcite and quartz (01/69), or of calcite with minor amounts of clinopyroxene and garnet (01/70). The fabric of the coarse-grained rock (>5 mm in grain size) is equigranular without preferred orientation. Garnet and clinopyroxene show a patchy distribution in the well-annealed fabric. The migmatite has muscovite, which indicates slightly lower metamorphic temperatures than at the other sample locations. Samples 01/63 (muscovite-rich) and 01/66 represent the migmatite. Metamorphic conditions were 570°C and 0.5 GPa (Table 1). The age of metamorphism is ~465 Ma (two calcsilicate rocks). The T_{DM} ages (eTable 2) are 1.7 Ga in the calcsilicate rocks (01/69, 01/70), 1.7 Ga and 1.8 Ga in migmatite (01/66, 01/63), and 1.9 Ga in amphibolite (01/67).

Sierra Umango

Migmatite with a marble layer (*c.* 20-100 m thick, lateral extension some km) and amphibolite (hornblende–plagioclase–quartz–garnet biotite in variable modes) layers (cm–m scale) locally intercalated with marble and calcsilicate rocks are the dominant lithologies. Samples are from 29°02′S; 68°46′W. The marble contains numerous tectonically eroded clasts (cm–m scale) of the surrounding sheared migmatite. The clasts are entrained in the calcite matrix without reaction textures around or in the clasts. Sample 01/77 is an example of the common migmatic gneiss (<15% feldspars, 40–50% quartz, <30% biotite, <5% muscovite, <5% garnet). The garnet is partially retrogressed with fine-grained rims of chlorite, biotite and muscovite. The muscovite may have formed during the shearing of the migmatite. Fine-grained amphibolite (>60% plagioclase, >20% hornblende, >10% biotite, <5% garnet and minor clinopyroxene, opaque minerals, titanite and apatite; 01/79) shows only one deformation. The clinopyroxene occurs locally with hornblende and biotite without reaction textures. Sample 01/80 is an undeformed (or completely recovered from deformation) marble (>90% calcite; <10% isolated grains of clinopyroxene, plagioclase, quartz, titanite) without preferred orientation in the equigranular fabric. Marble 01/89 from the same large outcrop has been deformed in a shear zone. Grain size of calcite is smaller than in marble 01/80 and the calcite grains have a preferred orientation. Peak metamorphic conditions were ~900°C and 0.95 GPa and 800°C and 0.9 GPa in amphibolite. The rim compositions of the minerals yielded ~750–800°C and 0.9 GPa and 770°C and 0.8 GPa, respectively (Table 1). The age of metamorphism (last recrystallization at high T in the marble) is ~420 Ma. The T_{DM} ages (eTable 2) are 1.7 Ga in the calcsilicate rocks (01/80, 01/89), 1.7 Ga in the migmatite (01/77) and 2.1 Ga in the amphibolite (01/79).

Sierra de Maz

Samples are from two sites at the eastern and one site at the western slope of the mountain range. In the eastern slope (Mina La Pampa; 29°13′S, 68°22′W), deformed migmatite (quartz, plagioclase, biotite, garnet in variable modes, 01/123, locally they contain sillimanite and potassic feldspar, 01/126) and plagioclase-rich orthogneiss are common. Orthogneiss is distinguished by up to 10-mm large plagioclase crystals in a finer-grained, polygonal matrix of plagioclase commonly with 120° grain boundary intersects in 01/124 (>70% plagioclase, <10% biotite, <5% garnet and hornblende). The Fe–Mg minerals are concentrated in layers, which mark the foliation and only minor amounts occur within the plagioclase matrix. Orthogneiss 01/129 (>60% plagioclase) shows clinopyroxene aggregates, which formed after up to 10 mm large single clinopyroxene crystals, still visible in the orientated trails of exsolution of opaque minerals. The aggregates are surrounded by an up to 1 mm wide rim of hornblende, minor biotite and garnet preferentially occurring within the rim. Calcsilicate rocks (01/125) show a polygonal fabric of >60% coarse-grained calcite, <20% clinopyroxene and epidote and <10 vol% plagioclase, amphibole and sericite grown after plagioclase. Layers of amphibolite (01/127) are closely

associated with calcsilicate rocks. The amphibolites (<35% plagioclase, <50% hornblende, <5% epidote and garnet) are characterized by thin layers of epidote with garnet. Amphiboles commonly show poikiloblastic textures with abundant inclusions of epidote and plagioclase from the matrix. Peak conditions of metamorphism recorded from the orthogneiss are ~750–800°C and 0.8–0.9 GPa. Rim compositions yield ~640–730°C and 0.7 GPa (Table 1). Discordant U–Pb ages from titanite yielded a lower intercept age of ~440 Ma and an upper intercept age of ~1,200 Ma, whereas U–Pb ages of ~430 Ma in a second sample are concordant (Lucassen and Becchio 2003). The T_{DM} ages (eTable 2) are 1.6 Ga in the calcsilicate rock (01/125), 1.6, 2.5 and 2.6 Ga in the migmatite, (01/127, 01/126, 01/123), 1.8 Ga in the amphibolite (01/118), and 1.8 and 2.1 Ga in the orthogneiss (01/129; 01/124).

At the northern end of the eastern slope of Sierra de Maz (29°10′S, 69°27′W), garnet-staurolite–muscovite–biotite-schist is the common rock type (01/101; >40% quartz, <30% biotite plus muscovite, <10% plagioclase, garnet and staurolite porphyroblasts). Micaschist (01/97, 01/98) with a higher amount of staurolite and abundant magnetite represents the transition to a layer (dm scale) of a magnetite-enriched metamorphic rock (01/99). The magnetite-rich rock contains patchy, disrupted opaque minerals (>40%) with zigzag grain boundaries in a matrix of ribbons formed by quartz, minor plagioclase, staurolite and biotite. Peak metamorphic conditions were ~650–700°C and 0.65 GPa from core compositions and low T of 560–620°C at slightly lower P of 0.5–0.6 GPa from rim compositions (Table 1). T_{DM} ages (eTable 2) are 1.8 and 2.4 Ga in micaschist (01/97, 01/101). The T_{DM} ages of 2.8 and 3.3 Ga in the magnetite-rich metamorphic rocks (01/98, 01/99) are among the highest in our sample set.

In the western slope (29°27′S, 68°30′W), sheared migmatite is the principal rock type, with minor amphibolite, marble and calcsilicate rocks. The internal preferred orientation marked by inclusions in garnet porphyroblasts of the amphibolites and mica schists is rotated with respect to the external foliation. Ages of metamorphism are ~440 and ~530 Ma. T_{DM} ages (eTable 2) are 1.7 Ga in amphibolite (01/108), 1.8 Ga in calcsilicate rock (01/111), and 2.0 Ga in sheared migmatite (garnet micaschist 01/105).

Element chemical and Sr, Nd and Pb isotope composition of the metamorphic basement

Element chemical composition

The rock types included in this study are variable in composition and comprise siliciclastic metasedimentary rocks (gneisses, migmatite, mica schist), carbonate-rich metasedimentary rocks (calcsilicate rocks to impure marble), two exotic iron-rich samples in the metasedimentary unit and metaigneous rocks (amphibolite, orthogneiss). Crust-normalized average major and trace element of gneisses, migmatite, and mica schist and the element distribution pattern of (para)gneisses and migmatites mostly from south of 27°S are very similar to formerly obtained data mainly from north of 27°S (Lucassen et al. 2001). The complete data set gives a reliable average composition of the basement, based on a total of ~300 analyses among them 48 paragneisses from the Puna and northern Sierras Pampeanas. The new data perfectly fit the pattern of the sedimentary and metasedimentary basement north of 27°S (major and trace element and isotope composition see eTable 2). A depletion of Na, Ca and Sr with respect to the average upper crust (Fig. 3a) occurs in many Early Palaeozoic felsic rocks of N Chile and NW Argentina and has been interpreted as an effect of one or more cycles of erosion and deposition of the respective source rocks (Lucassen et al. 2001). The average composition of the high-grade metamorphic basement is also similar to sedimentary rocks of the Puncoviscana Formation (Fig. 3a). The Puncoviscana Formation (e.g. Bock et al. 2000; Lucassen et al. 2001; Drobe et al. 2009) is considered to represent the protoliths of many metasedimentary rocks in NW Argentina (Schwartz and Gromet 2004; Büttner et al. 2005). The deviation of the average element pattern of the amphibolites from the average composition of the upper crust is less pronounced than the deviation of juvenile magmatic rocks (Fig. 3a).

The REE composition of gneisses, migmatite, and micaschist and the calcsilicate to impure marble largely overlap and the average compositions nearly coincide (Fig. 3c). This indicates a similar source of REE in siliciclastic and carbonate-dominated protoliths. REE distribution patterns of all metaigneous rocks are variably enriched in LREE (light REE; Fig. 3b). Prominent positive Eu anomalies are present in the two orthogneisses with high plagioclase contents from Sierra de Maz. The amphibolites show slightly negative or no Eu anomalies. The average REE composition of the amphibolite is more typical for arc-related rocks than for MORB (LREE depleted, lower REE contents) or intraplate magmatic rocks (higher contents, steeper REE pattern).

Isotope composition

Most new Nd and Sr isotope data of the metamorphic rocks (eTable 2) from the southernmost Puna plateau (Cazadero Grande; El Peñon), the western Sierras de Pampeanas and published compositions from metamorphic rocks of the southern plateau, northern Sierras Pampeanas (Lucassen et al. 2001) occupy the same compositional field (Fig. 4)

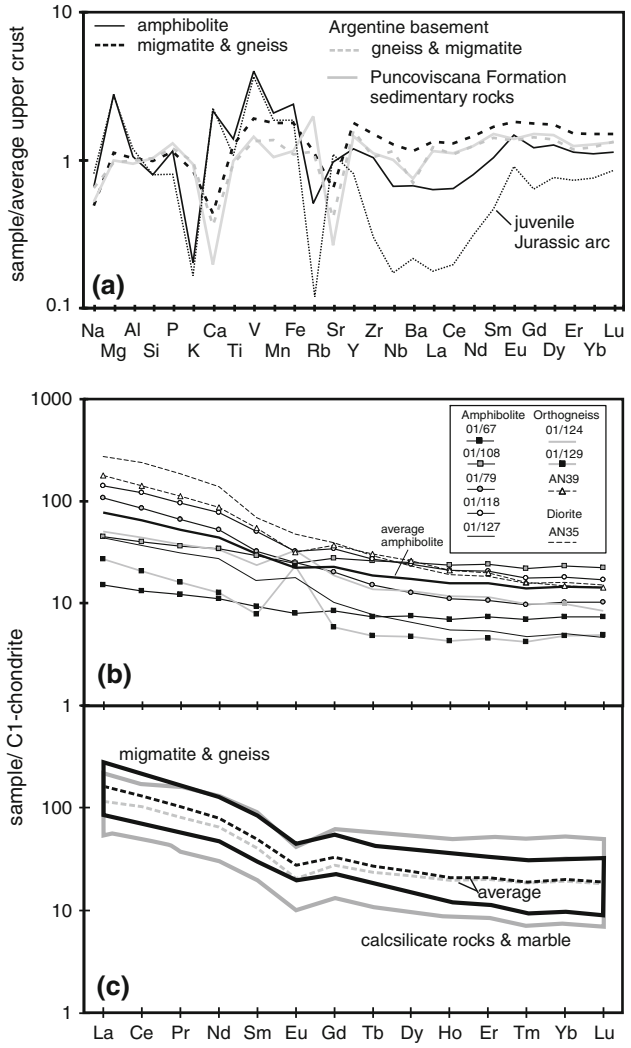

Fig. 3 **a** Average compositions of migmatite and gneiss from this study, compared with average gneiss and migmatite from Argentina and Puncoviscana Formation metasedimentary rocks ('Argentine basement'; Lucassen et al. 2001); values are normalized to average upper continental crust (Taylor and McLennan 1995). The basement in Argentina has a typical upper continental crust composition, except for Na–Ca–Sr contents (see text). Amphibolites from this study, which from the field observations are likely orthoamphibolites, are compared with the average composition of juvenile magmatic rocks from the Jurassic magmatic arc (Lucassen et al. 2006). Major element contents are similar, but trace elements vary significantly. **b**, **c** Chondrite-normalized REE pattern (C1 chondrite of Palme and O'Neill 2004) of **b** amphibolite and orthogneiss, **c** compositional fields and averages of calcsilicate rocks and marble and migmatite and gneiss

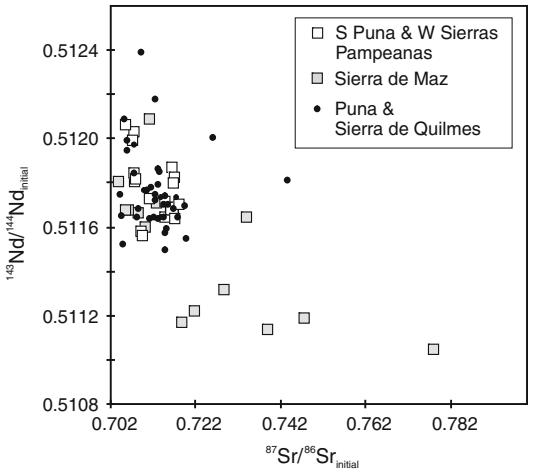

Fig. 4 Initial $^{87}Sr/^{86}Sr$ and $^{143}Nd/^{144}Nd$ of the southern Puna and western Sierras de Pampeanas and Sierra de Maz from this study compared with samples from the Puna and Sierra de Quilmes (Lucassen et al. 2001)

and are typical of the regional Palaeozoic continental crust. Metamorphic rocks from Sierras de Maz and Umango have lower Nd isotope ratios than the regional Palaeozoic continental crust. New T_{DM} ages (eTable 2) are summarized in Fig. 5.

The scatter of the initial Pb-isotope ratios of our whole-rock data is large and similar to feldspar and calcite from the same rock types and localities (Fig. 6, eTable 2; Lucassen and Becchio 2003). The ratios encompass the variability known from other Palaeozoic magmatic and metamorphic rocks from the Central Andes (discussion of the Pb variability in Lucassen et al. 2001, 2002; Mamani et al. 2008). The samples with low μ (<4) and the least radiogenic Pb isotope signatures (measured and age corrected to 500 Ma; eTable 2) are plagioclase-rich orthogneiss (01/124, 01/129) or amphibolite (01/118, 01/127) from Sierra de Maz. The unradiogenic $^{207}Pb/^{204}Pb$ and $^{206}Pb/^{204}Pb$ signatures of samples from Sierra de Maz coincide with those of the Arequipa massive, but $^{208}Pb/^{204}Pb$ of 01/127 and 01/129 is less radiogenic. The signature of these samples is similar to the composition from some Cambrian granite from ~24°S (Lucassen et al. 2002). A few samples, including the magnetite-rich 01/98, have initial $^{207}Pb/^{204}Pb$ that are higher than in other Palaeozoic rocks at comparable $^{206}Pb/^{204}Pb$. This indicates the influence of an old high-μ source in these samples (i.e. Early Proterozoic or Archean material enriched in U before exhaustion of the ^{235}U isotope, the parent of the stable ^{207}Pb), which is rare but known from the Central Andes (Fig. 6; eTable 2; Lucassen et al. 2002).

Discussion

Metamorphism and crystallization age

The pressure–temperature conditions of Early Palaeozoic metamorphic rocks from the study areas in N Chile and NW Argentina are in the range of ~0.4–1.0 GPa at temperatures between ~500 and 900°C (Table 1). Pressures of ~1.0 GPa at T ~800–900°C are restricted to Sierra

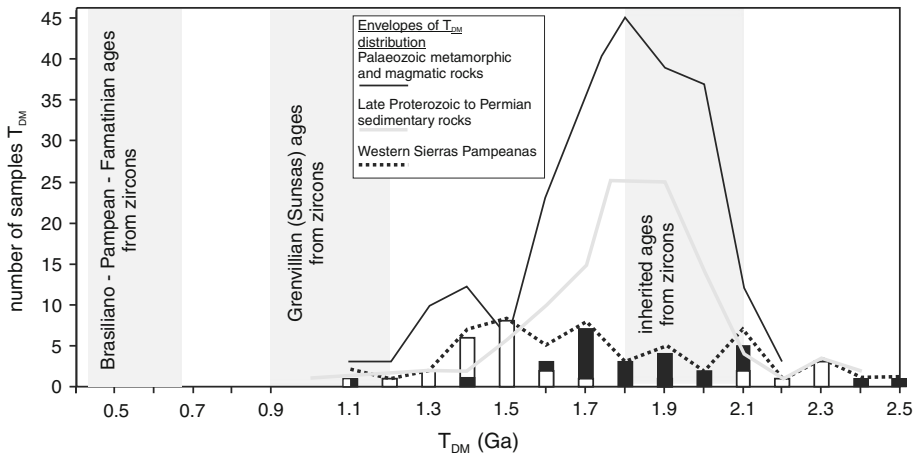

Fig. 5 Sm-Nd model ages (T_{DM}) compiled from this work and the literature, and the range of peaks in U–Pb ages from zircons (shaded area). Most T_{DM} of Palaeozoic metamorphic, magmatic and sedimentary rocks plot between 1.7 and 2.0 Ga. Our T_{DM} from the western Sierras Pampeanas (*black bars*) follows this pattern. Recently published data from the sierras de Maz and Espinal (*white bars*; Casquet et al. 2008) have a similar age range, but peak at somewhat younger ages. The black broken line 'Western Sierras Pampeanas' represents the total of both data sets. The U–Pb inheritance in zircons from Neoproterozoic to Late Palaeozoic rocks shows three peaks, one between 1.8 and 2.1 Ga, which coincides with the common T_{DM}, a second peak between 0.9 and 1.2 Ga, which represents the Sunsas (Grenville) orogeny, and a third one, which represents the Brasiliano–Pampean–Famatinian orogenies. The T_{DM} indicates only one major formation (or homogenization) of crust. All T_{DM} are recalculated to single-stage evolution model of Goldstein et al. (1984). *Data sources*: T_{DM} from the compilation in Lucassen et al. (2001) and Franz et al. (2006); additional data from Drobe et al. (2009). U–Pb data: Bahlburg et al. 2009; Damm et al. (1990, 1994), Wörner et al. (2000). Lucassen and Becchio (2003), Loewy et al. (2004), Steenken et al. (2006), Chew et al. (2007, 2008), Collo et al. (2009), Martin-Gombojav and Winkler (2008), Willner et al. (2008), Cardona et al. (2009), Casquet et al. (2010), Rapela et al. (2010), Zimmermann et al. (2010)

Umango (also previously observed by Porcher et al. 2004) and the southern part of Sierra de Maz. This corresponds to granulite facies conditions at lower crustal depth. Metamorphic conditions at the other locations are within the range of mid to upper amphibolite facies with temperatures commonly above the wet solidus of felsic compositions (~650°C; e.g. Johannes and Holtz 1996) and pressures between ~0.4 and 0.7 GPa. Felsic migmatite is a common rock type at most locations. High temperatures have extinguished information from the prograde path. Traces of retrograde metamorphism restrict to small rims around minerals that were influenced by element diffusion during cooling. The new *P–T* data are in accordance with metamorphic conditions described from other locations in N Chile (~18°S, Wörner et al. 2000) and from the Pampean and Famatinian of Argentina between ~26°S and 32°S (e.g. in Pankhurst and Rapela 1998; Hauzenberger et al. 2001; Porcher et al. 2004; Büttner et al. 2005; Otamendi et al. 2008). The peak metamorphic pressures correspond with two exceptions to crustal depth of 15–25 km. Indicators of continent collision in the metamorphic record, i.e., high pressure–low temperature rocks, appear to be absent in the Early Palaeozoic orogen, even in the presumed zone of Palaeozoic terrane accretion south of 30°S (e.g. Baldo et al. 1996; Lucassen et al. 2000; Büttner et al. 2005; Casquet et al. 2008; Delpino et al. 2007; Otamendi et al. 2008; Schwartz et al. 2008).

Age determinations on metamorphic minerals of the actual paragenesis are the direct link to metamorphic crystallization and deformation. The two groups of metamorphic crystallization ages of ~530–500 and ~470–420 Ma overlap spatially (Fig. 1). In N Chile, new and published age data from Belén, Mejillones, and Sierra de Moreno (~525, 505, 470, and 430 Ma) indicate the same age structure as in the southern Puna and its eastern slope (Lucassen et al. 2000; Wörner et al. 2000; Lucassen and Becchio 2003; Büttner et al. 2005) and in the Sierra de Maz–Sierra Umango area (Lucassen and Becchio 2003; Casquet et al. 2004; Porcher et al. 2004). Attempts to attribute a ~1.2 Ga age from metamorphic overgrowth on inherited older zircon to metamorphic conditions of ~780°C and 0.8 GPa in Sierra de Maz (Casquet et al. 2006) remain ambiguous, because two high T metamorphic overprints (at near identical P–T conditions as those reported by Casquet et al. 2006) occurred in the Cambrian and Late Ordovician–Silurian in Sierra de Maz.

Magmatism that is crustal-derived or contains high proportions of crustal material near-continuously occurs between ~570 and 440 Ma (e.g. Damm et al. 1990, 1994; in: Pankhurst and Rapela 1998; Pankhurst et al. 2000; Lucassen et al. 2001; Büttner et al. 2005; Chew et al. 2007; Viramonte et al. 2007) and requires thermal anomalies in the crust over the whole time span. Age spectra derived from detrital zircons from Late Palaeozoic (meta)

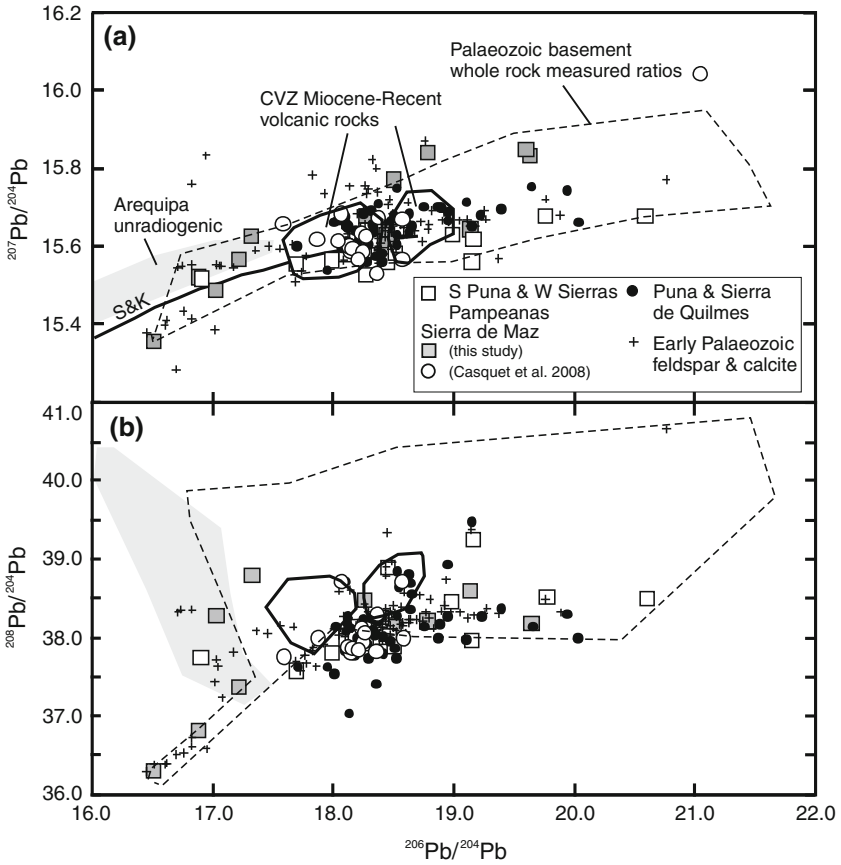

Fig. 6 Initial Pb isotope composition of whole-rock samples from southern Puna and western Sierras Pampeanas and Sierra de Maz from this study, data from Casquet et al. (2008) are from Sierras de Maz and Umango, whole-rock samples from Puna and Sierra de Quilmes, and feldspar and calcite data from Palaeozoic metamorphic and magmatic rocks (N Chile and NW Argentina; Lucassen et al. 2001, 2002; Lucassen and Becchio 2003). The field of Palaeozoic whole rock (N Chile and NW Argentina; Lucassen et al. 2001) and the samples of the Arequipa massif (Tilton and Barreiro 1980; compilation in Lucassen et al. 2002) are present-day values. Cenozoic volcanic rocks show two clusters of compositions (compilation in Lucassen et al. 2006 and abundant new data and map of distribution in Mamani et al. 2008). The regional distribution of the clusters indicates Pb provinciality (Mamani et al. 2008) related to the distribution of different crustal domains. The unradiogenic Midproterozoic Arequipa source is already an endmember in the compositional array of the Early Palaeozoic basement rocks. *S&K* indicates the crustal lead evolution from Stacey and Kramers (1975)

sedimentary rocks appear to be continuous from Pampean to Famatinian (e.g. Bahlburg et al. 2009; Willner et al. 2008). The spatial distribution and related to the huge area still sparse geochronological data does not unequivocally allow to distinguish between continuous high temperatures or episodes of thermal relaxation. In the eastern Sierras Pampeanas, metamorphism and magmatic activity ceased in the Early Ordovician (e.g. Siegesmund et al. 2010), but in the western Sierras Pampeanas, Southern Puna and N Chile, the Pampean and Famatinian ages show close spatial relations in the metamorphic rocks, without systematic differences in the metamorphic grades. Even if the gap in crystallization ages of the metamorphic rocks is not an artefact of sparse data, the gap was <30 Ma and the crust-lithosphere remained at high temperatures, because cooling of lithospheric sections by heat conduction is slow (10th of million years; e.g. Fowler 1990) and magmatism was still active. The occurrence of different concordant U–Pb ages on titanite in rock units without differences in the metamorphic grade or tectonic contacts has been interpreted as reset of the U–Pb clock by localized ductile deformation and recrystallization of the titanite during persistent high *T* (Lucassen and Becchio 2003).

Element and isotope chemical composition and crustal residence

The chemical affinities of Early Palaeozoic metasedimentary basement and granitoid intrusions, older Neoproterozoic to Cambrian sedimentary rocks and Ordovician sedimentary rocks indicate crustal recycling in sedimentary–magmatic cycles (e.g. Damm et al. 1990, 1994; Bock et al. 2000; Lucassen et al. 2001; Egenhoff and Lucassen 2003; Zimmermann and Bahlburg 2003; Zimmermann

et al. 2010). The new chemical data fit this scheme perfectly (Fig. 3). At the outcrop level, these felsic rocks are dominant and juvenile Early Palaeozoic additions to the crust, i.e. mafic magmatic rocks and their metamorphic or sedimentary equivalents are rare (above references). The small volumes of mafic magmatic and metamorphic rocks have chemical arc signatures and variable contributions from the felsic crust (e.g. Lucassen et al. 2001; Kleine et al. 2004; Coira et al. 2009). The plagioclase-rich orthogneiss and amphibolite from Sierra de Maz resemble compositional features of other metaigneous rocks from Sierra de Maz (Casquet et al. 2004; Rapela et al. 2010).

The Sm–Nd isotope system is used to constrain crustal residence ages. The distribution of the single-stage T_{DM} ages of Early to Late Palaeozoic metamorphic, magmatic and sedimentary rocks shows a prominent peak between 1.6 and 2.0 Ga (Fig. 5). The range of T_{DM} of our data and data from Sierra Umango (Varela et al. 2003) and Sierra de Maz (Casquet et al. 2008) coincides, but the latter peak at ca 1.5 Ga, whereas our data peak at ca 1.7 Ga (Fig. 5) with several samples of significantly older T_{DM}. This is likely the effect from accidental differences in the sampling of a relatively small area, because both data sets agree with the regional T_{DM} distribution, which is based on a much larger sample set (Fig. 5). The relations between U–Pb ages from zircons and crustal residence ages of Neoproterozoic to Late Palaeozoic sedimentary, metamorphic and magmatic rocks show interesting relations. The prominent peaks in zircon ages from a broad spectrum of Early to Late Palaeozoic rocks (Fig. 5) along the margin between Ecuador and Southern Chile are Palaeoproterozoic ($\sim$1.8–2.1 Ga), Grenvillian or Sunsas ($\sim$0.9–1.2 Ga), and Brasiliano—Pampean—Famatinian ($\sim$0.4–0.65 Ga). Older ages are rare in the zircon record. The T_{DM} and Palaeoproterozoic U–Pb ages largely overlap, but the T_{DM} ages are skewed towards somewhat younger ages down to 1.5 Ga. There are no important juvenile additions to the crust detected in the Sm–Nd system during the prominent Sunsas and Neoproterozoic to Early Palaeozoic orogenies, both well documented in the zircon ages. The major crust formation (or homogenization) occurred around 1.8–2.0 Ga. Subsequent orogenies recycled this crust. Minor juvenile additions could be hidden in the younger T_{DM} (<1.8 Ga), which possibly represent mixing between the Palaeoproterozoic and younger sources.

In Sierra de Maz, metasedimentary rocks have the oldest T_{DM} (2.4–2.8 Ga) in contrast to the T_{DM} (<2 Ga) from orthogneiss and amphibolite from the same area. Casquet et al. (2010) report the Sm–Nd isotope composition of five gneisses from the Arequipa massif, which yield T_{DM} of $\sim$2.5–2.8 Ga (recalculated to single-stage ages; Goldstein et al. 1984). The old residence ages could represent inheritance from the Early Palaeoproterozoic-Archean host of the younger igneous protoliths in agreement with previous interpretations (Casquet et al. 2008, 2010; Rapela et al. 2010). The εNd at 1,200 Ma, which is the presumable formation age of the igneous protolith of orthogneiss and amphibolite (Rapela et al. 2010), is between -1 and $+4$ for the metaigneous rocks of Sierra de Maz but negative for most metasedimentary rocks (-2 to -10). This indicates a depleted mantel component in the metaigneous rocks like elsewhere in metaigneous rocks of Sierra de Maz (Casquet et al. 2008; Rapela et al. 2010). The T_{DM} ages of 3.3 Ga for the magnetite-rich rock (sample 01–99) is not considered, because the $^{147}Sm/^{144}Nd$ of 0.15 is above typical crustal values (e.g. Goldstein et al. 1984) and a secondary change during metamorphism or during pre-metamorphic sedimentary-weathering processes cannot be precluded.

Pb-isotope compositions of metamorphic and magmatic rocks in the Central Andes are indicative of crustal domains due to the U mobility during Proterozoic metamorphism (e.g. Tilton and Barreiro 1980; Wasteneys et al. 1995; Tosdal 1996; Lucassen et al. 2002; Mamani et al. 2008). The Arequipa Pb signature with rather unradiogenic $^{207}Pb/^{204}Pb$ and $^{206}Pb/^{204}Pb$ (Fig. 6) is attributed to U depletion during Sunsas (Grenvillian) high-grade metamorphism. The second widespread Pb signature is more radiogenic than the Arequipa signature (Fig. 6) and represents the part of the same crust not depleted in U. Both signatures form a mixing array (Fig. 6). Both crustal sources contribute variably to the Pb signature of the Cenozoic Andean magmatism, which allows a spatial discrimination of dominance of one or the other source (Fig. 6; Mamani et al. 2008). The new analyses fit into this regional scheme (Fig. 6).

Peculiarities such as old high-μ signatures (high $^{207}Pb/^{204}Pb$ at given $^{206}Pb/^{204}Pb$) are of local importance only and have been tentatively explained as inheritance, i.e. not homogenized during the Sunsas or Early Palaeozoic orogenies (Lucassen et al. 2002).

At Sierra de Maz, correction of Pb isotope ratios for in situ decay to 1.2 Ga shifts Pb isotope ratios of most samples to the vicinity of the low μ orthogneiss and amphibolite (eTable 2). This indicates an early fractionation of the U/Pb ratio near the possible 1.2 Ga crystallization age (Casquet et al. 2004; Rapela et al. 2010) of the magmatic protoliths of orthogneiss and amphibolite.

Concluding remarks

Simultaneous thermal events in the crust are documented along the western margin of South America in the Early Palaeozoic (Fig. 1a). Metamorphic conditions were of high T and pressures between 0.4 and 0.7 GPa never exceeding 1.0 GPa. Early Palaeozoic low *T*–high *P* metamorphism,

i.e. eclogite facies, as known from the Alpine collision zones (e.g. Spalla et al. 1996) or of the Variscan orogen in Europe (e.g. O'Brien and Carswell 1993) is not described from the Palaeozoic of the Central Andes (e.g. Lucassen et al. 2000; Schwartz et al. 2008).

Radiogenic isotope compositions indicate a consistent compositional pattern. A main event of crustal formation (or homogenization) around 1.8–2.0 Ga is seen in the crustal residence ages and ages of inherited zircons of Early Palaeozoic metamorphic, magmatic and sedimentary rocks. The 2 Ga age is considered as a major event of crust formation around the Archean and Early Palaeoproterozoic core regions of South America (e.g. Cordani et al. 2000; Sato and Siga 2002; Rino et al. 2004), which may be in turn the source of Palaeoproterozoic–Archean remnants in the 2 Ga crust. Subsequent important growth stages were not detected in the Sm–Nd record despite well defined Sunsas (Grenvillian) and Neoproterozoic- Early Palaeozoic orogenies (thermal events) along the margin. The variable Pb-isotope composition is explained by U depletion during the Sunsas (Grenvillian) high-grade metamorphism, which can be traced in the Pb-isotope composition in such distant areas like Sierra de Maz (this work), N Chile (Belén; Wörner et al. 2000) and the Arequipa Massif of south Peru (Fig. 1; Tilton and Barreiro 1980; Tosdal 1996 and references therein). The contiguous Nd and Pb isotope signatures preclude the accretion of large volumes of material with depleted mantle signatures, e.g. island arcs, after the 2 Ga event.

In N Chile and NW Argentina ($\sim$18°–27°S), the belt of similar metamorphic conditions, crystallization ages, and composition extends eastwards from the Pacific coast to at least the eastern slope of the Puna. The spatial coherence of this section has been demonstrated from Neoproterozoic throughout the Phanerozoic (e.g. Damm et al. 1990, 1994; Lucassen et al. 1999a, 2000, 2001, 2002; Bock et al. 2000; Aceñolaza et al. 2002; Büttner et al. 2005; Franz et al. 2006; Zimmermann et al. 2010) and has been tentatively extended into the Sierras Pampeanas south of 27°S (Lucassen et al. 2000, 2001; Lucassen and Becchio 2003; Franz et al. 2006). Coherence in the evolution of the continental margin could be traced back from the Early Palaeozoic into the Proterozoic on a large regional scale at least between western Central Argentina (Sierras Pampeanas) to Ecuador by an increasing number of high precision age data on magmatic and metamorphic rocks and rapidly evolving provenance studies of zircons by in situ methods (e.g. Damm et al. 1990, 1994; Wörner et al. 2000; Lucassen and Becchio 2003; Loewy et al. 2004; Steenken et al. 2006, 2008; Chew et al. 2007, 2008; Collo et al. 2009; Martin-Gombojav and Winkler 2008; Willner et al. 2008; Cardona et al. 2009; Casquet et al. 2010; Rapela et al. 2010).

The segmentation of this margin by different Proterozoic–Late Palaeozoic terrane collisions in succession of the influential suggestion of Ramos et al. (1986) appears to be an ongoing issue (Ramos 2008). The uniform age structure of thermal events over large distances, uniform and consistent compositional trends are not in favour of collision of small, i.e. not margin-wide, exotic or para-autochthonous terranes in a subduction regime. Para-autochthonous terranes partially avoid the problem of disturbed compositional coherence, because they are from the same margin (Ramos 2008). However, they require a phase of continental rifting at the margin, ocean floor formation, and subsequent initiation of subduction and collision, if they can be considered a terrane. Continental break up commonly leads to important mantle-derived flood basalt magmatism that is not visible in the geological record of this margin. Collision should lead to high P metamorphism, i.e. the formation of blue-schist to eclogite facies rocks. Metamorphic conditions with T $\sim$700°C and P $\sim$1.3 GPa, which is the highest P reported from the Central Andes, in a small, isolated occurrence of Permian metamorphic rocks from the southern continuation of Sierra Moreno (Fig. 1) are certainly not indicative of collision-related metamorphism (Sierra de Limon Verde; Lucassen et al. 1999b). Extension along this margin of Gondwana is, a common, well-established feature, however. It resulted in large-scale sedimentary basins roughly parallel to the margin (for recent reviews: Tankard et al. 1995; Ramos 2000) at least in the Neoproterozoic-Cambrian (Puncoviscana Formation), Ordovician, Permian, and Cretaceous.

During Mesozoic to Early Tertiary time, extension triggered the formation of extensional to transpressional arcs along the Central Andes' margin (e.g. Scheuber and Reutter 1992; Scheuber and González 1999). This produced mainly juvenile magmas in the arc (e.g. Lucassen et al. 2006). Contemporaneously, small-volume intra-plate magmatism of mafic to ultramafic composition occurred in the back arc (e.g. Sempere et al. 2002; Lucassen et al. 2007; Comin-Chiaramonti et al. 2010). This magmatism contributed to the compositional variability of magmatic rocks at this margin without a fundamental change of the overall composition of the crust (Franz et al. 2006). The further elaboration of a model for the Neoproterozoic to late Palaeozoic history of metamorphism–magmatism–sedimentation considering oscillation of the margin between extensional, transpressional and compressional phases (e.g. Bahlburg et al. 2009; Büttner 2009) without fragmentation and (exotic) terrane accretion could lead to an alternative to the presently dominant 'accretion model'.

Acknowledgments We thank F. Galbert (TU-Berlin), O. Appelt and D. Rhede (Deutsches GeoForschungsZentrum) for help with the

electron microprobes; M. Lewerenz (TU-Berlin) for the XRF analyses; P. Dulski and B. Zander for ICP- MS analyses and C. Schulz for help with the sample preparation for TIMS (all at Deutsches GeoForschungsZentrum); R. L. Romer for providing advice during the U–Pb data acquisition and critical reading of the manuscript. Reviews of C. Augustsson and V. Ramos improved the manuscript. The study was funded by the German Research foundation (DFG) in the frame of SFB 267 "Deformation Processes in the Andes", a DAAD travel grant to F. L., a DAAD grant and CONICET PIP 6103 to R. B., who also thanks FONCYT–PICT 07-38131 and CIUNSa for support.

References

Aceñolaza FG, Toselli AJ (1976) Consideraciones estratigráficas y tectónicas sobre el Paleozoico inferior del noroeste argentino. 2° Congreso Latinoamericano de Geología, Caracas. Actas 2:755–763

Aceñolaza FG, Miller H, Toselli AJ (2002) Proterozoic–early paleozoic evolution in western South America—a discussion. Tectonophysics 352:121–137

Astini RA, Dávila FM (2004) Ordovician back arc foreland and Ocloyic thrust belt development on the western Gondwana margin as a response to Precordillera terrane accretion. Tectonics 23. doi:10.1029/2003TC001620

Baeza L (1984) Petrography and tectonics of the plutonic and metamorphic complexes of Limon Verde and Mejillones Peninsula, northern Chile. PhD. thesis, Eberhard-Karl Universität, Tübingen, pp 1–205

Bahlburg H, Vervoort JD, Du Frane SA, Bock B, Augustsson C, Reimann C (2009) Timing of crust formation and recycling in accretionary orogens: Insights learned from the western margin of South America. Earth Sci Rev 97:215–241

Baldo EG, Demange M, Martino RD (1996) Evolution of the Sierras de Cordoba, Argentina. Tectonophysics 267:121–146

Becchio R (2000) Petrología y geoquímica del basamento del borde oriental de la Puna Austral. PhD. thesis, Universidad Nacional de Salta, Argentina, pp 1–183

Becchio R, Lucassen F, Franz G, Viramonte J, Wemmer K (1999) El basamento paleozoico inferior del noroeste de Argentina (23–27°S)—metamorfismo y geocronologia. In: Bonorino GG, Omarini R, Viramonte J (eds) Geologia del noroeste Argentino. XIV Congreso Geológico Argentino, Salta, Argentina, Relatorio, pp 58–72

Berman RG (1988) Internally-consistent thermodynamic data for stoichiometric minerals in the system Na_2O–K_2O–CaO–MgO–FeO–Fe_2O_3–Al_2O_3–SiO_2–TiO_2–H_2O–CO_2. J Petrol 29:445–522

Berman RG (1991) Thermobarometry using multi-equilibrium calculations: a new technique, with petrological applications. Can Mineral 29:833–855

Bhattacharya A, Mohanty L, Maji A, Sen SK, Raith M (1989) Non-ideal mixing in the phlogopite–annite binary: constraints from experimental data on Mg–Fe partitioning and a reformulation of the biotite–garnet geothermometer. Contrib Mineral Petrol 111:87–93

Bock B, Bahlburg H, Wörner G, Zimmermann U (2000) Tracing crustal evolution in the southern Central Andes from Late Precambrian to Permian using Nd and Pb isotopes. J Geol 108:515–535

Büttner SH (2009) The Ordovician Sierras Pampeanas—Puna basin connection: basement thinning and basin formation in the Proto-Andean back-arc. Tectonophysics 477:278–291

Büttner SH, Glodny J, Lucassen F, Wemmer K, Erdmann S, Handler R, Franz G (2005) Ordovician metamorphism and plutonism in the Sierra de Quilmes metamorphic array: Implications for the tectonic setting of the northern Sierras Pampeanas (NW Argentina). Lithos 83:143–181

Cardona A, Cordani UG, Ruiz J, Valencia VA, Armstrong R, Chew D, Nutman A, Sanchez AW (2009) U-Pb zircon geochronology and Nd isotopic signatures of the pre-Mesozoic metamorphic basement of the eastern Peruvian Andes: growth and provenance of a Late Neoproterozoic to Carboniferous accretionary orogen on the northwest margin of Gondwana. J Geol 117:285–305

Casquet C, Rapela CW, Pankhurst RJ, Galindo C, Dahlquist J, Baldo EG, Saavedra J, González Casado JM, Fanning CM (2004) Grenvillian massif-type anorthosites in the Sierras Pampeanas. J Geol Soc Lond 162:9–12

Casquet C, Pankhurst RJ, Fanning CM, Baldo E, Galindo C, Rapela CW, González-Casado JM, Dahlquist JA (2006) U–Pb SHRIMP zircon dating of Grenvillian metamorphism in Western Sierras Pampeanas (Argentina): correlation with the Arequipa Antofalla craton and constraints on the extent of the Precordillera Terrane. Gondwana Res 9:524–529

Casquet C, Pankhurst RJ, Rapela CW, Galindo C, Fanning CM, Chiaradia M, Baldo E, González-Casado JM, Dahlquist J (2008) The Mesoproterozoic Maz terrane in the Western Sierras Pampeanas, Argentina, equivalent to the Arequipa–Antofalla block of southern Peru? Implications for West Gondwana margin evolution. Gondwana Res 13:163–175

Casquet C, Fanning CM, Galindo C, Pankhurst RJ, Rapela C, Torres P (2010) The Arequipa massif of Peru: new SHRIMP and isotope constraints on a Paleoproterozoic inlier in the Grenvillian orogen. J S Am Earth Sci 29:128–142

Cawood PA, Buchan C (2007) Linking accretionary orogenesis with supercontinent assembly. Earth Sci Rev 82:217–256

Chew DM, Kosler J, Whitehouse MJ, Gutjahr M, Spikings RA, Miskovic A (2007) UPb geochronologic evidence for the evolution of the Gondwanan margin of the north-central Andes. Geol Soc Am Bull 119:697–711

Chew D, Schaltegger U, Kosler J, Magna T, Whitehouse MJ, Kirkland C, Miskovic A, Cardona A, Spikings RA (2008) U–Pb geochronologic evidence for the Neoproterozoic—Palaeozoic evolution of the Gondwanan margin of the North-Central Andes. In: 27th International Symposium on Andean Geodynamics (Nice), Extended Abstracts, pp 120–123

Coira B, Davidson J, Mpodozis C, Ramos V (1982) Tectonic and magmatic evolution of the Andes of northern Argentina and Chile. Earth Sci Rev 18:303–332

Coira B, Kirschbaum A, Hongn F, Pérez B, Menegatti N (2009) Basic magmatism in northeastern Puna, Argentina: chemical composition and tectonic setting in the Ordovician back-arc. J S Am Earth Sci 28:374–382

Collo G, Astini RA, Cawood PA, Buchan C, Pimentel M (2009) U–Pb detrital zircon ages and Sm–Nd isotopic features in low-grade metasedimentary rocks of the Famatina belt: implications for late Neoproterozoic–early Palaeozoic evolution of the proto-Andean margin of Gondwana. J Geol Soc 166:303–319

Comin-Chiaramonti P, Lucassen F, Girardi VAV, De Min A, Gomes CB (2010) Lavas and their mantle xenoliths from intracratonic Eastern Paraguay (South America Platform) and Andean Domain, NW-Argentina: a comparative review. Miner Petrol (in press). doi: 10.1007/s00710-009-0061-6

Cordani UG, D'Agrella-Filho MS, Brito-Neves BB, Trindade RIF (2003) Tearing up Rodinia: the Neoproterozoic palaeogeography of South American cratonic fragments. Terra Nova 15:350–359

Cordani UG, Teixeira W, D'Agrella-Filho MS, Trindade RIF (2009) The position of the Amazonian Craton in supercontinents. Gondwana Res 15:396–407

Damm KW, Pichowiak S, Harmon RS, Todt W, Kelley S, Omarini R, Niemeyer H (1990) Pre-Mesozoic evolution of the central

Andes; the basement revisited. Geol Soc Am Special Pap 241:101–126
Damm KW, Harmon RS, Kelley S (1994) Some isotope and geochemical constraints on the origin and evolution of the Central Andean basement (19°–24°S). In: Reutter KJ, Scheuber E, Wigger PJ (eds) Tectonics of the Southern Central Andes. Springer, Heidelberg, pp 263–275
Delpino SH, Bjerg EA, Ferracutti GR, Mogessie A (2007) Counterclockwise tectonometamorphic evolution of the Pringles metamorphic complex, Sierras Pampeanas of San Luis (Argentina). J S Earth Am Sci 23:147–175
Drobe M, López de Luchi MG, Steenken A, Frei R, Naumann R, Siegesmund S, Wemmer K (2009) Provenance of the late Proterozoic to early Cambrian metaclastic sediments of the Sierra de San Luis (Eastern Sierras Pampeanas) and Cordillera Oriental, Argentina. J S Am Earth Sci 28:239–262
Egenhoff SO, Lucassen F (2003) Chemical and isotopic composition of lower to upper Ordovician sedimentary rocks (Central Andes/South Bolivia): implications for their source. J Geol 111: 487–497
Finney SC, Peralta SH, Gehrels GE, Marsaglia K (2005) The Early Paleozoic history of the Cuyania (greater Precordillera) terrane of western Argentina: evidence from geochronology of detrital zircons from Middle Cambrian sandstones. Geol Acta 3:339–354
Fowler CMR (1990) The solid Earth. Cambridge University Press, Cambridge, pp 1–472
Franz G, Lucassen F, Kramer W, Trumbull RB, Romer RL, Wilke H-G, Viramonte JG, Becchio R, Siebel W (2006) Crustal evolution at the Central Andean continental margin: a geochemical record of crustal growth, recycling and destruction. In: Oncken O, Chong G, Franz G, Giese P, Götze H-J, Ramos VA, Strecker MR, Wigger P (eds) The Andes: active subduction orogeny. Frontiers in earth sciences, vol 1. Springer, Heidelberg, pp 45–64
Ghent ED, Stout MZ (1981) Geobarometry and geothermometry of plagioclase-biotite-muscovite assemblages. Contrib Mineral Petrol 76:92–97
Goldstein SL, ONions RK, Hamilton PJ (1984) A Sm–Nd study of atmospheric dust and particulates from major river systems. Earth Planet Sci Lett 70:221–236
Graham CM, Powell R (1984) A garnet-hornblende geothermometer: calibration, testing and application to the Pelona Schist, Southern California. J Met Geol 2:13–31
Grissom GC, Debari SM, Page SE, Page RE, Villar LM, Coleman RG, de Ramirez MV (1991) The deep crust of an early Paleozoic arc; The Sierra de Fiambala, northwestern Argentina. In: Harmon RS, Rapela CW (eds) Andean magmatism and its tectonic setting. Geol Soc Am Spec Pap 265:189–200
Grissom GC, DeBari SM, Snee LW (1998) Geology of the Sierra Fiambalá, northwestern Argentina: implications for Early Palaeozoic Andean tectonics. In: Pankhurst RJ, Rapela CW (eds) The Proto-Andean Margin of Gondwana. Geol Soc London Spec Pub 142:297–332
Hauzenberger ChA, Mogessie A, Hoinkes G, Felfernig A, Bjerg EA, Kostadinoff J, Delpino SY, Dimieri L (2001) Metamorphic evolution of the Sierras de San Luis: granulite facies metamorphism related to mafic intrusions. Mineral Petrol 71:95–126
Holdaway M, Mukhopadhyay B, Dyar M, Guidotti C, Dutrow B (1997) Garnet-biotite geothermometry revised: new Margules parameters and a natural specimen data set from Maine. Am Mineral 82:582–595
Holland T, Blundy J (1994) Non-ideal interactions in calcic amphiboles and their bearing on amphibole-plagioclase thermometry. Contrib Mineral Petrol 116:433–447
Johannes W, Holtz F (1996) Petrogenesis and experimental petrology of granitic rocks. Springer, Berlin, pp 1–335
Kleemann U, Reinhardt J (1994) Garnet-biotite thermometry revisited: the effect of Al^{vi} and Ti in biotite. Eur J Mineral 6:925–941
Kleine T, Mezger K, Zimmermann U, Münker C, Bahlburg H (2004) Crustal evolution of the early Ordovician Proto-Andean margin of Gondwana: trace element and isotope evidence from Complejo Igneo Pocitos (Northwest Argentina). J Geol 112:503–520
Kohn MJ, Spear FS (1990) Two new geobarometers for garnet amphibolites, with applications to southeastern Vermont. Am Mineral 75:89–96
Kraemer B, Adelmann D, Alten M, Schnurr W, Erpenstein K, Kiefer E, van den Bogaared P, Goerler K (1999) Incorporation of the Paleogene foreland into the Neogene Puna plateau: the Salar de Antofalla area, NW Argentina. J S Am Earth Sci 12:157–182
Lindsley DH (1983) Pyroxene thermometry. Am Mineral 68:477–493
Loewy SL, Connelly JN, Dalziel IWD (2004) An orphaned basement block: the Arequipa-Antofalla basement of the central Andean margin of South America. Geol Soc Am Bull 116:171–187
Lucassen F, Becchio R (2003) Timing of high-grade metamorphism: early Paleozoic U-Pb formation ages of titanite indicate long-standing high-T conditions at the western margin of Gondwana (Argentina, 26–29°S). J Metamorphic Geol 21:649–662
Lucassen F, Franz G, Thirlwall MF, Mezger K (1999a) Crustal recycling of metamorphic basement: late Paleozoic granites of the Chilean coast range and Precordillera at 22°S. J Petrol 40:1527–1551
Lucassen F, Franz G, Laber A (1999b) Permian high pressure rocks—the basement of Sierra de Limón Verde in N-Chile. J S Am Earth Sci 12:183–199
Lucassen F, Becchio R, Wilke HG, Thirlwall MF, Viramonte J, Franz G, Wemmer K (2000) Proterozoic–Paleozoic development of the basement of the Central Andes (18°–26°)—a mobile belt of the South American craton. J S Am Earth Sci 13:697–715
Lucassen F, Becchio R, Harmon R, Kasemann S, Franz G, Trumbull R, Wilke HG, Romer RL, Dulski P (2001) Composition and density model of the continental crust at an active continental margin—the Central Andes between 21° and 27°S. Tectonophysics 341:195–223
Lucassen F, Harmon R, Franz G, Romer RL, Becchio R, Siebel W (2002) Lead evolution of the Pre-mesozoic crust in the Central Andes (18°–27°): progressive homogenisation of Pb. Chem Geol 186:183–197
Lucassen F, Kramer W, Bartsch V, Wilke H-G, Franz G, Romer RL, Dulski P (2006) Nd, Pb, and Sr isotope composition of juvenile magmatism in the mesozoic large magmatic province of northern Chile (18–27°S): indications for a uniform subarc mantle. Contrib Mineral Petrol 152:571–589
Lucassen F, Franz G, Romer RL, Schultz F, Dulski P, Wemmer K (2007) Pre-cenozoic intra-plate magmatism along the Central Andes (17–34°S): composition of the mantle at an active margin. Lithos 99:312–338
Maksaev V (1990) Metallogeny, geological evolution, and thermochronology of the Chilean Andes between latitudes 21° and 26° south, and the origin of the major porphyry copper deposits. Unpublished PhD thesis, Dalhouse University, Halifax, Nova Scotia, Canada, 555 pp
Mamani M, Tassara A, Wörner G (2008) Composition and structural control of crustal domains in the central Andes. Geochem Geophys Geosyst 9. doi:10.1029/2007GC001925
Martin-Gombojav N, Winkler W (2008) Recycling of Proterozoic crust in the Andean Amazon foreland of Ecuador: implications for orogenic development of the Northern Andes. Terra Nova 20:22–31
Massonne HJ, Schreyer W (1987) Phengite geobarometry based on the limiting assemblage with K-feldspar, phlogopite, and quartz. Contrib Mineral Petrol 96:212–224

Miller H, Toselli AJ, Rossi de Toselli J, Aceñolaza FG (1994) Regional and geochronological development of the metamorphic basement in Northwest Argentina. Zentralblatt Geologie Paläontologie Teil1 (Heft 1/2):263–273

O'Brien PJ, Carswell DA (1993) Tectonometamorphic evolution of the Bohemian massif: evidence from high pressure metamorphic rocks. Geologische Rdsch 82:531–555

Otamendi JE, Tibaldi AM, Vujovich GI, Viñao GA (2008) Metamorphic evolution of migmatites from the deep Famatinian arc crust exposed in Sierras Valle Fértil–La Huerta, San Juan, Argentina. J S Am Earth Sci 25:313–335

Palma M, Parica P, Ramos V (1986) El granito de Archibarca: su edad y significado tectónico, provincia de Catamarca. Rev Asoc Geol Argent 41:414–419

Palme H, O'Neill HStC (2004) Cosmochemical estimates of Mantle Composition. In: Holland HD, Turrekian KK (eds) Treatise on geochemistry 2, pp 1–38. Elsevier, Amsterdam, The Netherlands

Pankhurst RJ, Rapela CW (1998) The Proto-Andean margin of Gondwana. Geol Soc Lond Spec Pub 142:383 pp

Pankhurst RJ, Rapela CW, Saavedra J, Baldo E, Dahlquist J, Pascua I, Fanning CM (1998) The Famatinian magmatic arc in the southern Sierras Pampeanas. In: Pankhurst RJ, Rapela CW (eds) The Proto-Andean Margin of Gondwana. Geol Soc Lond Spec Pub 142:343–367

Pankhurst RJ, Rapela CW, Fanning CM (2000) Age and origin of coeval TTG, I- and S-type granites in the Famatinian Belt of the NW Argentina. In: Barbarin B, Stephens WE, Bonin B, Bouchez JL, Clarke D, Cuney M, Martin H (eds) Fourth Hutton symposium on the origin of granites and related rocks. Trans Royal Soc Edinburgh Earth Sci 91:151–168

Pankhurst RJ, Rapela CW, Fanning CM, Márquez M (2006) Gondwanide continental collision and the origin of Patagonia. Earth Sci Rev 76:235–257

Porcher CC, Fernandes LAD, Vujovich GI, Chernicoff CJ (2004) Thermobarometry, Sm/Nd ages and geophysical evidence for the location of the suture zone between Cuyania and the western Proto-Andean margin of Gondwana. Gondwana Res 7:1057–1076

Ramos VA (2000) The Southern Central Andes. In: Cordani UG, Milani EJ, Thomaz-Filho A, Campos DA (eds) Tectonic evolution of South America: Rio de Janeiro, 31st International Geological Congress, 561–604

Ramos VA (2008) The basement of the Central Andes: the Arequipa and related terranes. Annu Rev Earth Planet Sci 36:289–324

Ramos VA, Jordan TE, Allmendinger RW, Mpodozis C, Kay SM, Cortés JM, Palma MA (1986) Palaeozoic terranes of the central Argentine Chilean Andes. Tectonics 5:855–880

Rapela CW, Pankhurst RJ, Casquet C, Baldo E, Saavedra J, Galindo C, Fanning CM (1998) The Pampean Orogeny of the southern proto-Andes: evidence for Cambrian continental collision in the Sierras de Córdoba. In: Pankhurst RJ, Rapela CW (eds) The Proto Andean margin of Gondwana. Geol Soc Lond Spec Pub 142:181–217

Rapela CW, Pankhurst RJ, Casquet C, Baldo E, Galindo C, Fanning CM, Dahlquist JM (2010) The Western Sierras Pampeanas: protracted Grenville-age history (1330–1030 Ma) of intra-oceanic arcs, subduction-accretion at continental edge and AMCG intraplate magmatism. J S Am Earth Sci 29:105–127

Rino S, Komiy T, Windley BF, Katayama I, Motoki A, Hirata T (2004) Major episodic increases of continental crustal growth determined from zircon age of river sands: implications for mantle overturns in the early Precambrian. Phys Earth Planet Ints 146:369–394

Romer RL (2001) Lead incorporation during crystal growth and the misinterpretation of geochronological data from low-$^{238}U/^{204}Pb$ metamorphic minerals. Terra Nova 13:258–263

Romer RL, Rötzler J (2001) P–T–t evolution of ultrahigh-temperature granulites from the Saxon Granulite Massif, Germany. Part II: geochronology. J Petrol 42:2015–2032

Romer RL, Rötzler J (2005) Effect of metamorphic reaction history on the U–Pb dating of titanite. Geol Soc Lond Spec Pub 220: 147–158

Sato K, Siga O Jr (2002) Rapid growth of continental crust between 2.2 and 1.1 Ga in the South American Platform: integrated Australian, European, North American and SW USA crustal evolution study. Gondwana Res 5:165–173

Scheuber E, González G (1999) Tectonics of the Jurassic Early Cretaceous magmatic arc of the north Chilean Coastal Cordillera (22°–26°S): a story of crustal deformation along a convergent plate boundary. Tectonics 18:895–910

Scheuber E, Reutter K-J (1992) Magmatic arc tectonics in the Central Andes between 21° and 25°S. Tectonophysics 205:127–140

Schwartz J, Gromet P (2004) Provenance of a late Proterozoic to early Cambrian basin, Sierras de Córdoba, Argentina. Precambrian Res 129:1–21

Schwartz J, Gromet P, Miro R (2008) Timing and duration of the calc-alkaline arc of the Pampean orogeny: implications for the late Neoproterozoic to Cambrian evolution of western Gondwana. J Geol 116:39–61

SEGEMAR (Servicio Geologico y Minero Argentino) (1997) Mapa geológico de la República Argentina, scale 1: 250000. Secretaria de Industria Comercio y Mineria de Argentina, Buenos Aires

Sempere T, Carlier G, Soler P, Fornari M, Carlotto V, Jacay J, Arispe O, Néraudeau D, Cárdenas J, Rosas S, Jiménez N (2002) Late Permian–Middle Jurassic lithospheric thinning in Peru and Bolivia, and its bearing on Andean-age tectonics. Tectonophysics 45:153–181

Sengupta P, Dasgupta S, Bhattacharya PK, Hariya Y (1989) Mixing behavior in quaternary garnet solid solution and an extended Ellis and Green garnet-clinopyroxene geothermometer. Contrib Mineral Petrol 103:223–227

Siegesmund S, Steenken A, Martino RD, Wemmer K, López de Luchi MG, Frei R, Presnyakov S, Guereschi A (2010) Time constraints on the tectonic evolution of the Eastern Sierras Pampeanas (Central Argentina). Int J Earth Sci (Geol Rundsch). doi: 10.1007/s00531-009-0471-z

Sims JP, Ireland TR, Camacho A (1998) U–Pb, Th–Pb and Ar–Ar geochronology from the southern Sierras Pampeanas, Argentina: implications for the Palaeozoic tectonic evolution of the western Gondwana margin. In: Pankhurst RJ, Rapela CW (eds) The Proto Andean margin of Gondwana. Geol Soc Lond Spec Pub 142:259–282

Spalla MI, Lardeaux JM, Dal Piaz JV, Gosso G, Messiga B (1996) Tectonic significance of Alpine eclogites. J Geodynamics 21:257–285

Stacey JS, Kramers JD (1975) Approximation of terrestrial lead isotope evolution by a two-stage model. Earth Planet Sci Lett 26:207–221

Steenken A, Siegesmund S, López de Luchi MG, Frei R, Wemmer K (2006) Neoproterozoic to Early Palaeozoic events in the Sierra de San Luis: implications for the Famatinian geodynamics in the Eastern Sierras Pampeanas (Argentina). J Geol Soc 163:965–982

Steenken A, Siegesmund S, Wemmer K, López de Luchi MG (2008) Time constraints on the Famatinian and Achalian structural evolution of the basement of the Sierra de San Luis (Eastern Sierras Pampeanas, Argentina). J S Am Earth Sci 25:336–358

Tankard AJ, Suárez Soruco R, Welsink HJ (1995) Petroleum basins of South America. AAPG Memoir 62:792

Taylor SR, McLennan SM (1995) The geochemical evolution of the continental crust. Rev Geophys 33:241–265

Tilton GR, Barreiro BA (1980) Origin of lead in Andean calcalkaline lavas, southern Peru. Science 210:1245–1247

Tosdal RM (1996) The Amazon–Laurentian connection as viewed from the middle Proterozoic rocks in the central Andes, western Peru and northern Chile. Tectonics 15:827–842

Varela R, Sato AM, Basei MAS, Siga O Jr (2003) Proterozoico medio y Paleozoico inferior de la sierra de Umango, antepaís andino (29°S), Argentina: edades U-Pb y caracterizaciones isotópicas. Revista Geológica de Chile 30:265–284

Viramonte JM, Becchio R, Viramonte JG, Pimentel MM, Martino R (2007) Ordovician igneous and metamorphic units in southeastern Puna: new U–Pb and Sm–Nd data and implications for the evolution of northwestern Argentina. J S Am Earth Sci 24:167–183

Wasteneys HA, Clark AH, Farrar E, Langridge RJ (1995) Grenvillian granulite-facies metamorphism in the Arequipa Massif, Peru; a Laurentia-Gondwana link. Earth Planet Sci Let 132:63–73

Willner AP, Gerdes A, Massonne H-J (2008) History of crustal growth and recycling at the Pacific convergent margin of South America at latitudes 29°-36°S revealed by a U-Pb and Lu-Hf isotope study of detrital zircon from late Paleozoic accretionary systems. Chem Geol 253:114–129

Wörner G, Lezaun J, Beck A, Heber V, Lucassen F, Zinngrebe E, Rößling R, Wilke HG (2000) Geochronology, metamorphic petrology and geochemistry of basement rocks from Belén (N. Chile) and C. Uyarani (W. Bolivian Altiplano): Implications for the evolution of Andean basement. J S Am Earth Sci 13:717–737

Zimmermann U, Bahlburg H (2003) Provenance analysis and tectonic setting of the Ordovician clastic deposits in the southern Puna Basin, NW Argentina. Sedimentology 50:1079–1104

Zimmermann U, Niemeyer H, Meffre S (2010) Revealing the continental margin of Gondwana: the Ordovician arc of the Cordón de Lila (northern Chile). Int J Earth Sci (Geol Rundsch). doi:10.1007/s00531-009-0483-8